Pergamon

Planet. Space Sci., Vol. 44, No. 8, pp. 749–782, 1996

0032–0633/96 $15.00+0.00

PII: S0032-0633(96)00013-X

Amounts of crustal stretching in Valles Marineris, Mars

Daniel Mège and Philippe Masson

Laboratoire de Géologie Dynamique de la Terre et des Planètes, URA CNRS D 1369, Université Paris-Sud, Orsay, France

Received 16 November 1994; revised 20 December 1995; accepted 20 December 1995

Abstract. Terrestrial grabens and continental rifts are compared with the Valles Marineris system, in order to define the mechanisms which could be responsible for its geometry and formation. Simple shear/pure shear mechanisms, symmetric/asymmetric grabens and faults, high/low dip angles, block tilting/no block tilting, shouldering or not, lithospheric layering, and amount of sedimentation on chasma floors are discussed. Amounts of stretching on several transverse topographic profiles are then calculated, assuming either block tilting or no block tilting. On each profile initial dip angles ranging from 40° to 90°, and sediment thicknesses ranging from 0 to 3 km are considered, as well as symmetric and asymmetric border fault dips. The case of Ius Chasma, the southwestern trough of the Valles Marineris system, is first considered, then the entire graben system. Considering a constant 660 km profile length, stretching increases eastward in Ius Chasma from the Noctis Labyrinthus boundary (stretching factor $\beta = 1.01$–1.02, assuming initial 60° dipping faults) to the middle part of this trough ($\beta = 1.04$–1.06). Then Ius Chasma stretching decreases, but is partly taken over by stretching in Candor and Ophir chasmata. Stretching decreases from the eastern part of Melas Chasma ($\beta = 1.05$–1.06) to almost the eastern end of Coprates Chasma ($\beta = 1.01$). Then stretching increases again eastward ($\beta = 1.02$–1.04) at the longitude Coprates Chasma splits around a horst and Gangis Chasma opens northward. A striking feature is that a low peak of extension in the centre of the Valles Marineris troughs is observed ($\beta = 1.03$–1.04). The low stretching peak in the central part of Valles Marineris may originate from the existence of buried structures in the grabens, and/or along-strike variations in sediment thickness. According to the profiles and to the hypotheses, some 9–26 km of additional normal movements along faults with dip angles equivalent to the dip angles of the walls would be expected within the central Valles Marineris grabens to get constant stretching from Ius to Coprates chasmata. The amount of this lacking offset may be partly explained by a few km subsidence of Ophir Planum, and the shallow inter-chasmata grabens. Part of the remaining lacking normal movements are best explained by buried structures (possibly shallow horst and graben alternances or other structures) in the major canyons: Melas, Candor, and/or Ophir chasmata—probably mainly in Melas Chasma. Alternatively, along-strike variations of sediment thickness (about 3 km) without taking such buried structures into account, can explain the results as well. Observation of images shows up that the most realistic structural model of Valles Marineris should probably consider both variations of sediment thicknesses and existence of buried structures. Models for the origin of Valles Marineris stretching are discussed. The role of passive rifting in crust weakened by hot spot is emphasized, although extensional stresses due to the Tharsis load should have also contributed to stretching. Copyright © 1996 Elsevier Science Ltd

1. Introduction

Valles Marineris (Fig. 1) is located on the eastern side of the Martian Tharsis bulge. It includes several troughs of structural origin (see some of the main structures on Fig. 2), hundreds of km long, tens of km wide, and 4–10 km deep, whose major deepening stage dates back to Hesperian (Tanaka, 1986; Scott and Tanaka, 1986; Lucchitta *et al.*, 1992; Peulvast *et al.*, 1996). In this study we discuss in detail the comparison with terrestrial rifts, and attempt to obtain more accurate indications in calculating the amount of Valles Marineris crustal stretching under a wide range of plausible parameters. We first consider series of grabens bounded by planar faults, slipping without tilting, and then the effects of possible block tilting are added. Both methods are likely rudimentary compared with the graben complexity.

Correspondence to: D. Mège

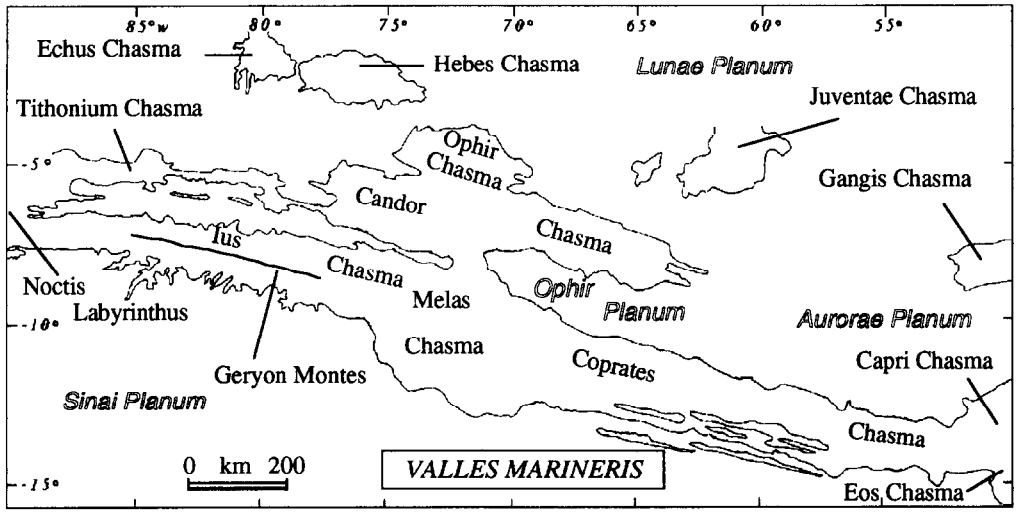

Fig. 1. Toponymic map of Valles Marineris

1.1. *Previous works*

Structural analysis, and, frequently, comparison with terrestrial rifts, have been investigated by Mutch *et al.* (1976), Blasius *et al.* (1977), Masson (1977, 1980, 1985), Frey (1979), Carr (1981), Schultz (1991, 1995), Anderson and Grimm (1994, 1995), Mège (1994), Mège and Masson (1994a, b), Kiefer and Johnson (1995), and Peulvast *et al.* (1996). The structural pattern analyses carried out by Masson (1977) both in Valles Marineris and the East African Rift revealed similarities between these two regions. The conclusions of Schultz (1991) include the possibility of gentle northward tilt of the Coprates Chasma floor, and the existence of systematic altitude differences between plateaus located north and south of both Ius and Coprates chasmata. The northern plateaus lie above the 8 km level, whereas the southern ones currently lie at 8 km or less. These observations are consistent

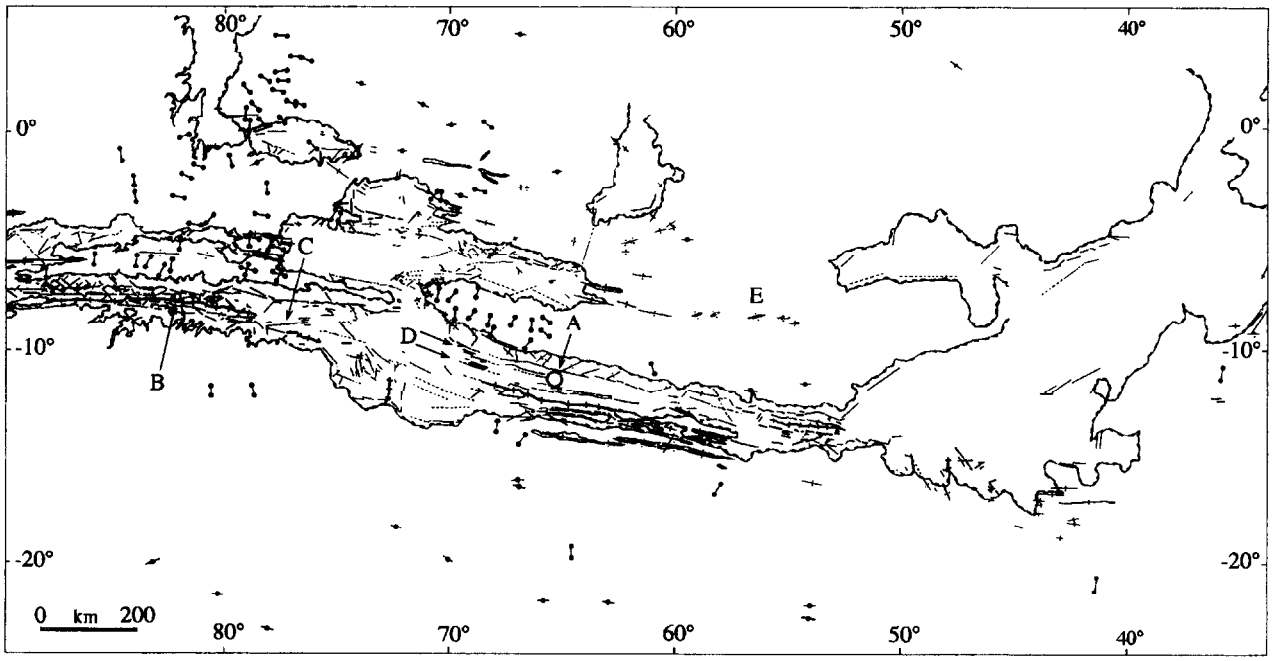

Fig. 2. Very simplified structural map of Valles Marineris. Lines: faults; stippled lines: suspected faults; lines with two thin dots, left and right: vertical fractures mainly shown up as zones of weakness (pit chains, sapping channels, oblique troughs on wallslopes); lines with thick dots on both ends: the line trends give local extensional direction inferred by some narrow grabens on plateaus; lines with thick dots in the middle: the line trends give local contractional directions inferred from some wrinkle ridges. The thick lines cut by perpendicular segments in the canyons show the main crest lines. A, B: Location of two large impact craters on the floor of Ius and Coprates chasmata, perhaps directly formed on plateau materials before Valles Marineris subsidence. C: Buried structures east of Geryon Montes underlined by dark fissural lava flows. D: Border faults of minor horsts in the western part of Coprates Chasma. E: *En échelon* vertical joints underlining the gradual reorientation of the Valles Marineris structure from the N105°E westward trend toward the E/W trend observed in Gangis Chasma

with block tilting in terrestrial rifts. Valles Marineris would have first developed asymmetrically with north major border faults dipping southward, evolving further in a more symmetric way, the other faults developing as synthetic or antithetic faults. Moreover, the structural division of Ius Chasma presents some analogy with terrestrial continental rift division (Peulvast *et al.*, 1996). An asymmetric structure is also expected in other Valles Marineris troughs, including Coprates (Schultz, 1991) and Candor chasmata (Mège and Masson, 1994a).

In order to explain the structural asymmetry, Schultz (1991) investigated the possibility of a deep detachment fault, noting that this would result in a detachment level more than 90 km deep, involving a very thick brittle crust. He did not dismiss the possibility of planar major normal faults, a hypothesis which is also consistent with structural asymmetry.

Detailed quantification of stretching across the Valles Marineris chasmata has not been attempted yet before this study and the parallel study by Schultz (1995). The style of rifting in Valles Marineris, i.e. wide (Basin and Range type) or narrow (East African rift type) has been investigated by Anderson and Grimm (1994, 1995), and Kiefer and Johnson (1995). Attempts of calculating crustal stretching on the northern Tharsis region were made by Carr (1974) and Plescia (1991).

1.2. *Can Valles Marineris reasonably be a rift?*

Strictly speaking, Valles Marineris (like most of the extensional structures on planetary surfaces except the Earth's surface) is unable to be treated as terrestrial rifts since the latter are consequences of horizontal traction of rigid plates, mostly due to subduction pull and that temptative subduction of the Martian crust is still not predicted by any audacious but realistic evolution model of Mars (Pruis and Tanaka, 1995). However, for conveniency, the following text will consider that rifts are sites of crustal breaking, whatever the basic processes involved.

Mechanisms alternative to the rift interpretation have been suggested—the most quoted one was presented by Tanaka and Golombek (1989)—but encounter some difficulty with rock mechanics (Schultz, 1991, 1992) and morphostructural observations (Mège, 1994; Mège and Masson, 1996b).

Tanaka and Golombek (1989) rejected the rift hypothesis for two main reasons. First, terrestrial rifts are not associated with pit chains. This argument is not valid for the following reasons. On Earth, oceanic rifting is usually associated with dyke swarm emplacement. Dyke swarms form first, and influence the location of the border faults of the future rift (Fahrig, 1987). The existence of buried dykes can be suspected in remote sensing studies when subsurface ice or water in the bedrock interact with magma, resulting in surface phenomena along the dyke propagation path such as thermokarstic depressions (Squyres *et al.*, 1987; Costard, 1990a, b; Costard and Kargel, 1995; Davis *et al.*, 1995), and explosive eruptions (Lorenz, 1986) under some pressure condition and when the water content in the bedrock is close to 0.35% (Sheridan and Wohletz, 1981; Kokelaar, 1986). Structural effects may also arise when dykes are shallow enough. Dyke emplacement has a wedging effect on the bedrock above the dyke top (see pp. 152–153 of Anderson (1951)) which can participate to crustal stretching if the remote stress is also extensional (Opheim and Gudmundsson, 1989; Rubin, 1990; Forslund and Gudmundsson, 1991; Gudmundsson, 1995). Dykes are also density and strength discontinuities which focus the remote stress (e.g. Zoback, 1992). All these mechanisms have been shown by Mège and Masson (1995b, 1996b) to have played a role in the formation of some pits and troughs aligned with the chasmata, suggesting analogy with alignment of dyke swarms and normal faults in some terrestrial rifts.

The second reason is that the Valles Marineris structure would not be complex enough. This is not confirmed by detailed mapping (Fig. 2, and Mège (1991), Peulvast and Masson (1993), and Peulvast *et al.* (1996)). The main characteristics of terrestrial rifts also include a structural asymmetry, which was shown to exist in Valles Marineris in the works mentioned above and in Schultz (1991). Another characteristic in terrestrial continental rifts is the existence of transfer zones on Earth, which include several categories of oblique structural trends (Gawthorpe and Hurst, 1993). Although this is not the main purpose of this paper, some kinds of transfer zones should also exist in Valles Marineris. Of particular interest is the case of some transfer faults which sometimes shift the main border faults from one side of a graben to the other side. Although transfer faults exist in Valles Marineris, such a shift appears not to exist. They reactivate ancient major lineaments in the basement on Earth (Precambrian shear zones for instance; e.g. Villeneuve (1983), Rosendahl (1987), Chorowicz *et al.* (1988, 1989), Chorowicz (1989), Daly *et al.* (1989), Maurin and Guiraud (1993), and Piper (1989)). Therefore many of them could not exist without large horizontal block movements. In Valles Marineris, their absence may be directly linked with the lack of plate tectonics. Thus the structural complexity appears not to be a suitable argument against the rift hypothesis in the Valles Marineris case.

The following section compares the structural features of the terrestrial rifts with those of Valles Marineris in order to better investigate the mechanisms of crustal stretching. This will also help to quantify the parameters required to calculate the amount of stretching (Section 3). The main results are then presented (Section 4) and discussed (Section 5).

2. Mechanisms and geometry of terrestrial rifts and Valles Marineris

Calculation of stretching implies the definition of plausible graben geometries. To this end, some preliminary points should be discussed, including the amount of sedimentation in troughs, the location of the main faults, the fault throws, and the fault dips. We first discuss in detail the possible rifting mechanisms and the geometry of Valles Marineris, in comparison with terrestrial rifts. The following aspects are considered: pure shear/simple shear

thinning, symmetric/asymmetric border faults, listric/planar faults, steep/gentle dips, lithospheric layering.

2.1. *Thinning process (pure shear/simple shear)*

Although thinning at the lithospheric scale is obviously completed by pure shear, at the crust scale, two end-member mechanisms for thinning may take place: pure shear (McKenzie, 1978) or simple shear (Wernicke, 1985).

Rosendahl (1987) synthesized a rift evolution model. Before possible oceanization, the asymmetry is developed from the earliest tectonic stage by lithospheric simple shear following Wernicke's model. The rift has a half graben geometry, which tends to evolve to a rather symmetric geometry shortly before oceanization.

Geometrical considerations led Morley (1989) to define two kinds of rifts in the East African Rift System. The first type (e.g. Lake Tanganyika rift) presents high angle fault dips in the upper crust, which deformed by pure shear. The lower ductile crust is deformed by pure shear as well; nevertheless it may consist of distributed, anastomosing simple shear zones. This mechanism lasts until the crust has been stretched by several kilometres. In more evolved rifts, such as the Kenya rift, pure shear in the lower crust would be abandoned with stretching increase. A low angle detachment would develop from the anastomosing simple shear zone in the ductile crust. Once this step is reached, this mechanism would be suitable to accommodate tens or hundreds of km extension. At the end, the whole crust is dominated by simple shear, which simultaneously affects deeper and deeper levels in the lithosphere, reaching the bottom of the lithospheric mantle.

Another example is provided by the Oslo rift, where the upper crustal stretching factor (defined as the final length/initial length ratio in a stretched area) averages $\beta = 1.4$ (Klemperer, 1988). Simple shear is developed in the upper crust and in the upper mantle, suggesting that such a moderate extension may be enough for simple shear to be significant. In the Rhenish rift, the limited extension observed may be completed by pure shear (Ziegler, 1992a). However, Brun *et al.* (1992) estimated from deep seismic reflection data that a low angle detachment might exist from the upper crust to the lithospheric mantle, with a possible gap within the lower crust. It should be noted indeed that the existence of low angle detachments involving the whole lithosphere has not been as frequently demonstrated as popularized (see other examples in Klemperer (1988) and Keen *et al.* (1989)).

What happened in the Valles Marineris lithosphere? In order to discuss possible processes analogous to those in terrestrial rifts, it is important to ensure that the thickness of the crust prior to rifting was similar, because this parameter influences the amount of stretching required to develop simple shear. Most of the deformation occurred prior to the deposit of stratified materials and during the period of development of the spur and gully morphology (Lucchitta *et al.*, 1992). The location of spurs and gullies (especially those displaying faceted spurs) gives a good idea on the location of walls on which most of the tectonic events occurred. However, it is not possible yet to infer fault behaviour at depth and thus to define how far is the stretching level advanced, and calculation of the stretching factor will provide an idea on the dominant shear process in the crust when Valles Marineris stretching stopped. If the usually considered ~ 50 km thick "normal" current Martian crust is correct, and if the scenarios of thermal evolution predicting monotonous planetary cooling and crust thickening with time (e.g. Schubert *et al.*, 1992) are correct, then the mean current terrestrial crust thickness (≈ 30 km) may be a good approximation for Mars when Valles Marineris formed, about 2 or 3 Gy ago (Neukum and Wise, 1976; Hartmann *et al.*, 1981).

2.2. *Graben geometry (symmetric/asymmetric)*

A general structural asymmetry between one main border fault and antithetic border faults is a frequent feature of terrestrial rifts. It develops and grows up from the earliest stages of rift evolution, and extends throughout the process (Morley, 1989).

Pure shear allows asymmetric rifts to form, basically because mechanically, stress and strain focus on a number of crustal discontinuities inversely dependent on their spacing (Nur, 1982). This asymmetry generally leads to half graben development, like for instance in the East African Rift System (e.g. Rosendahl, 1987; Hetzel and Strecker, 1994), West and Central African Rift System (see references in Maurin and Guiraud (1993)), Oslo rift (Ziegler, 1992b), Rhenish rift (Brun *et al.*, 1992) and, more generally, basins belonging to the Southwestern European Rift System (Bois, 1993). In the Baikal Rift System, Logatchev (1993) attributes the half graben geometry to three possible processes: asymmetric mantle upwelling, reactivation of Precambrian and Paleozoic thrust zones, and location of the rift system at the edge of the Siberian craton. It is of interest also to notice that recent works on the Kenya rift structure put forward the same four characteristics: half graben geometry, asymmetric asthenospheric rise, reactivation of old (Pan-African) structures, and location on a suture zone between two lithospheric units (Archean Tanzania Craton and Proterozoic Mozambique Belt) (Hetzel and Strecker, 1994). An asymmetric upwelling is also considered by Melosh and Williams (1989) to explain the asymmetric structure of some terrestrial rifts. We point out that even without these circumstances asymmetry in continental rifts may merely develop from the fact that all the faults are in the same strain field: strain focuses on a number of faults inversely proportional to the distance between the faults, favouring the formation of a single major fault in a rift cross-section.

A structural asymmetry is observed in some Valles Marineris troughs where the northern walls of Ius Chasma (Peulvast *et al.*, 1996; Mège, 1991), Coprates Chasma (Schultz, 1991), and Candor Chasma (Mège and Masson, 1994b) underwent more extensional deformation than the southern walls. However, both image interpretation and topographic analyses strongly argue against half graben structures. Reactivation of ancient structures and location

on a suture zone are not supported by observations (Mutch *et al.* (1976) and subsequent works). Existence of possible links with asymmetric asthenospheric upwelling is of course very speculative.

2.3. *Fault geometry (high angle/low angle; planar/listric)*

2.3.1. *Slope angles of the Valles Marineris fault scarps.* The dips of the major faults in Valles Marineris cannot be deduced from image interpretation, because of the high but unclear amount of erosion. If we assume a homogeneous crust, the Anderson model is valid and the first fault will be 60° dipping. But the possible occurrence of inherited fractures leads to modify this model. Previous fractures, formed as parts of the Tharsis radial fracture system, existed before the opening of Valles Marineris, during the Noachian and lower Hesperian (e.g. Scott and Tanaka, 1986). All the previous interpretations of this radial fracture system (Mutch *et al.*, 1976; Schultz and Glicken, 1979; Wise *et al.*, 1979; Plescia and Saunders, 1982) imply that these fractures are vertical (Carr, 1981). The initial fractures of Valles Marineris were part of this network, as deep tension fractures (Tanaka and Golombek, 1989) or intruded joints (Mège and Masson, 1995b, 1996b). Our calculations must then consider the case for very steep dips at the initiating stage of graben formation.

If we assume that the Geryon Montes horst initially reached the same elevation as the surrounding plateaus (8.5 km) at the middle of Ius Chasma, where it passes over the 7 km elevation, and was then eroded without significant subsiding, a constraint can be put on the minimal fault dips of the border faults north and south of Geryon Montes. The distance between both of them implies that their minimum dips averaged 40°, possibly 50°; and assuming 60° dips, the initial width of Geryon Montes would average 10 km. Some other minimum dip values calculated from photogrammetric analyses in Valles Marineris are presented by Chadwick and Lucchitta (1992), and range from 46° to 70°. However, these faults are not border faults, and their genesis and evolution may have not been the same. Higher values (52°–86°) have been found for trough-wall faults that parallel the long axis of the troughs (Chadwick and Lucchitta, 1993). However the faults measured by Chadwick and Lucchitta (1993) could be representative of narrow radial graben faults, but not representative of chasma faults. The difference could be appreciable if the mechanism for chasma formation is different from that of narrow graben formation (see discussion and Schultz (1995)).

We attempted to measure the dip angle of the faceted spurs and other recent fault scarps located at the bottom of the border faults, from comparison between high resolution pictures and the experimental detailed topographic map of Ius and Tithonium chasmata (USGS, 1980). We found that the current slopes could be as low as 20–40°. These low values do not prevent steep initial dips. On Earth, under semi-arid conditions, fault scarps evolve following the equation of diffusion (Nash, 1980), which states that the variation of elevation is proportional to the slope curvature: $\delta z/\delta t = C(\delta^2 z/\delta x^2)$, where t represents time, z and x are the vertical axis and the horizontal axis perpendicular to the slope of the scarp, respectively. C ($m^2 y^{-1}$) is a constant, assuming that the cohesion of slope material is negligible and particle properties are uniform. The scarp angle diminishes under the control of gravity and may typically reach 35°. The further scarp evolution is wash-controlled and the scarp may reach values within the 25–8° range (Wallace, 1977). On Earth, 20–35° are particularly stable under favourable geomorphological conditions, and slopes ranging between 25 and 35° can be preserved for a few million years (Wallace, 1978). The current dips of the Martian faceted spurs are thus not indicative of the initial fault dips, and, in particular, not inconsistent with steep border faults.

2.3.2. *Initial dip angles of the Valles Marineris border faults.* Possible values for the initial dip angles of the Valles Marineris border faults must be discussed in order to define which ones should be included in the stretching calculations. A simple hypothesis is considering that all the faults have a 60° initial dip. This hypothesis was used for a number of stretching calculations across shallow Martian grabens, from some of the oldest works (Carr, 1974) to very recently (Davis *et al.*, 1995). For the Valles Marineris grabens, although this hypothesis may be correct, a wider range of dips should be considered to account for different models of fault initiation.

Steep dips (>70°). Some models involving formation of the border faults from vertical joints, together with the results obtained by Chadwick and Lucchitta (1993), require very steep initial faults. In extensional regions on Earth such as Iceland, the normal faults develop from vertical tension fractures (Gudmundsson, 1992). Tension fractures form at the surface with a small length, and, individually or by coalescence, grow in length and depth for several hundred metres. At a typical depth range of 0.5–1.5 km a throw begins to develop and the tension fracture progressively becomes a steeply dipping normal fault (Bäckström and Gudmundsson, 1989; Gudmundsson and Bäckström, 1991; Forslund and Gudmundsson, 1992) whose throw linearly increases as a function of length (Gudmundsson, 1992). Measurements on 315 faults by Forslund and Gudmundsson indicated that the dip range is 42–89°, 80% are within the range 65–79°, and the mean dip is 73°. The maximum vertical throws are several hundreds of metres, and there seems to be a correlation between the maximum vertical throw increase and the dip angle decrease (from 89° to 73°). Thus in case of faults forming from vertical joints, one can suggest that the dips rapidly decrease to 70° (they would probably reach 60° if the throws were larger). This agrees with the results by Brun and Choukroune (1983) shown on Fig. 3. Models involving intruded joints (Carr, 1974; Mège and Masson, 1995a, b, 1996b) require such steeply dipping initial faults as well.

"Classic" dips (60°). The case for initial 60° dipping faults corresponds to models based on the Anderson rule (Anderson, 1951). This rule is adapted to the assumption of newly formed faults in fractured crust. Numerous works on crustal stretching have assumed 60° dipping normal faults; in Valles Marineris, this value was assumed in the model proposed by Tanaka and Golombek (1989). In this model, the faults would have developed above deep

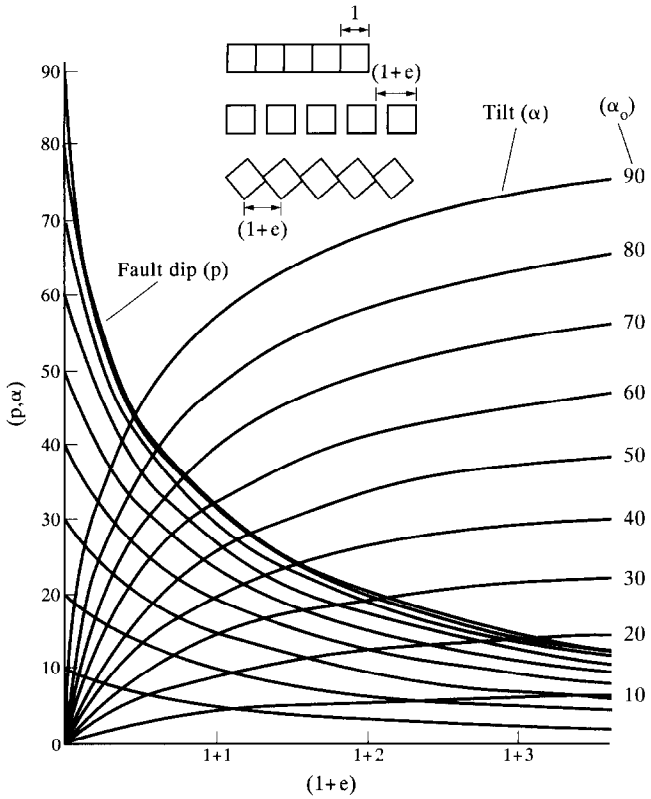

Fig. 3. Fault dip p and block tilt α variations as a function of finite stretch $(1+e)$. Initial values of p (p_0) and α (α_0) are indicated (Brun and Choukroune, 1983)

tension cracks. The crack upper tips would correspond to the depth of fault initiation, ruling out possible analogy with the Icelandic rift.

Moderate dips ($<50°$). Low angle initial normal faults may result from inheritance of low angle discontinuities in the crust. This case is encountered on Earth when old thrusts are reactivated (Jackson and McKenzie, 1983; Daly *et al.*, 1989). This requires large-scale horizontal block movements, and cannot apply to Valles Marineris, as previously stated. A few studies (Plescia and Golombek, 1986; Zuber, 1995) have suggested that the wrinkle ridges could involve low angle faulting of much of the Martian crust. Since wrinkle ridges are observed in the Valles Marineris surrounding plateaus, and formed earlier than Valles Marineris, low angle discontinuities could have influenced its development if these interpretations are correct. However, the wrinkle ridges are mostly perpendicular to the Valles Marineris grabens (Chicarro *et al.*, 1985; Watters and Maxwell, 1986), and thus could not have been reactivated as border faults.

Without considering the stress field, dyke intrusion creates a local extensional field (e.g. Pollard, 1987). If a global remote stress field is accounted for, Parsons and Thompson (1993) showed that the superimposition of both fields favours the development of low angle normal faults above the dykes. Therefore, models involving dyke emplacement parallel to Valles Marineris should also take possible low angle faults into account if the emplacement of some dykes was contemporaneous to the formation of nearby normal faults.

Consequently, we consider that the initial dips of the Valles Marineris border faults ranged from 90° (inherited faults from previous vertical joints, consistent with results obtained by Chadwick and Lucchitta (1993)), to 60° (newly formed faults in Anderson's model), and to 40° (normal fault initiation contemporaneous to, and influenced by, vertical dyke emplacement).

2.3.3. *Evolution of fault geometry.* Once a range of initial dips has been defined, it is necessary to examine if fault rotation occurred or not, i.e. to determine whether the dip angles remained constant throughout stretching or whether they were lowered. Ultimately, large rotations contribute to form listric faults and, subsequently, low angle detachments. Schultz (1991) discussed either the possibility of listric and planar major faults but does not side with any of them. The development of listric faults and detachments on Earth appears to be closely related to horizontal traction and heat flow.

Individual fault geometry has been subject to numerous discussions since the early 1980s. Dresen *et al.* (1991) showed from analogue and numerical modelling that planar faults form by subsidence in isotrope material. This was shown along either 90° or 60° dipping basement faults. Conversely, horizontal traction favours the development of listric faults. Under horizontal traction, planar faults get a curved shape due to block tilting (Jackson and McKenzie, 1983). Jackson (1987) suggested that the steeply dipping planar faults in the upper crust may also undergo a diminution of the dip angle in a small transitional brittle–ductile zone between the upper crust and the lower crust. Listric faults evolve into low angle or flat detachments with increasing stretching.

The style of propagation of faults at depth appears to be also dependent on the thickness of the brittle upper lithospheric layer, i.e. on heat flow (Buck, 1988, 1993; Morley, 1989). If the heat flow is weak (leading to a thick brittle crust), the fault is steeply dipping and may cut the entire brittle upper part of the lithosphere. Conversely, high thermal gradient (leading to a thin brittle crust) in regions of extension is responsible for major fault flattening at depth, and connecting them with a subhorizontal detachment. In detail, the lower part of the steep fault may be abandoned and absorbed in the ductile crust the top of which is rising. The higher part of the fault keeps active and its dip angle slightly decreases. It prolongates at depth, following a new low dip trend. Connecting all the low angle faults leads to a low angle or flat detachment (Morley, 1989), such as in metamorphic core complexes, which may move upward or downward according to the initial distance between the initial normal faults, compared with the detachment depth, and to basin infill and loading (Barr, 1987).

Since plate tectonics does not exist on Mars, large horizontal tractions are unlikely. Horizontal stresses from planetary cooling, which might have an effect at the time of formation of Valles Marineris are compressive and hydrostatic and thus cannot produce large-scale horizontal movements and replace the effect of plate tectonics. Similarly, the wrinkle ridge trends cannot have been induced by Valles Marineris stretching (e.g. Watters and Maxwell, 1986; Watters, 1993). Therefore, following Dresen *et al.* (1991), if listric faults formed in Valles Marineris, their development should have remained embry-

onic. Moreover, Valles Marineris does not look like core complexes, as also pointed out by Anderson and Grimm (1994). The virtual detachment depth calculated by Schultz in Coprates Chasma, assuming a 8 km offset, 60° dip and a tilting angle less than 3° (close to the maximum value for Coprates Chasma allowed considering that the poorly constrained topography is horizontal) would be 90 km. Since detachments occur in the case of thin crusts, the depth calculated by Schultz (1991) tends to argue against a major detachment beneath Valles Marineris.

2.4. *Fault rotation*

Listric faults are not expected to have developed in Valles Marineris, however, before planar faults become listric, horizontal stretching needs and produces block rotation: (1) it is an intrinsic geometrical necessity in elastic crust stretching. Horizontal extension is achieved by vertical thinning: pure shear results from a combination of simple shear and rotation (Jackson and McKenzie, 1983; Jackson, 1987). (2) An additional component of rotation is required to account for field observations, and is due to the lithospheric response to thinning. The latter rotation component is especially observed on rift borders where it leads to footwall uplift. In the subsequent part of the text "stretching rotations" and "lithospheric response to thinning" will be distinguished to account for these two sets of mechanisms.

2.4.1. *Stretching rotation.* Since block tilting has been generally investigated in the case of "domino" block geometry (like in core complexes), its validity for "full" grabens should be discussed. In the case of horizontal traction ("passive" rifting on Earth), rotation on one border fault in a full graben (i.e. in the early stages stretching, before the development of significant asymmetry) may be counteracted by the attempt of the antithetic border faults to rotate in the opposite sense, and finally no rotation may result (Fig. 4a, c). In this early stage, the lithospheric uplift due to unloading is estimated to be negligible, contrary to later stages during which lithospheric uplift induces fault rotation.

Conversely, in the case of crustal stretching induced by vertical forces (mantle upwelling; "dynamic" or "active" rifting on Earth), important extensional forces are expected to be distributed under the entire extended area. One fault may not absorb all the extensional forces underlying the rift. Each movement produced on one fault does not counteract movement on other faults (Fig. 4b, d). Block rotation may occur. After rift initiation, this difference between passive and active rifting becomes less important because passive rifting induces vertical uplift, and dynamic rifting becomes mainly accommodated by horizontal stretching. Therefore block rotation should be possible in both configurations. An important factor determining if block rotation can have taken place in Valles Marineris is thus the amount of stretching: for rather small stretching, rotation may have been impeded; for more advanced stretching, block rotation is likely to have occurred.

2.4.2. *Lithospheric response to thinning.* It is here assumed that lithospheric response to thinning does not produce additional extension. Jackson (1987) mentions the case of the Gulf of Mexico and Niger Delta, where vertical readjustment of the margin produced stretching in the up-dip direction and shortening in the down-dip direction, in such a way that the net stretching is null. This is an important point because otherwise the lithospheric response to thinning should be taken into account in calculating the stretching factor. This would require the assumption of some highly speculative values on various parameters, such as the lithospheric thickness in the Valles Marineris region at the time of tectonic activity.

As a consequence of this mechanism, tilting due to the lithospheric response to its thinning is responsible for overestimating the dip angle variation on faults produced by stretching. Morley (1989) studied the possible influence of footwall uplift in the Kenya rift case. The component of dip variation during extension due to footwall uplift is as high as 10 . The fact that the lithospheric response to thinning lowers the dip angle is not important for the stretching estimations here since the calculations will not consider the observed fault dips, because intense wall erosion occurred and the current slopes do not reflect fault dips. Nevertheless its influence on rotation of the Valles Marineris border faults is important to consider, because it may partly explain the discrepancy between the current slopes and the fault dips that will be modelled in the next section, together with wall erosion.

A clue to that past rotation induced by the lithospheric response to thinning should have taken place in Valles Marineris is illustrated below. Footwall uplift has a controversial origin, but necking due to buoyant forces resulting from basin unloading appears to be an essential process (Weissel and Karner, 1989; Kusznir *et al.*, 1991). Other mechanisms (for instance isostatic uplift caused by underplating, and dynamic uplift due to convection) may play a role as well, which in some cases is supported by geophysical data, but in some other cases is not (van der Beek *et al.*, 1994).

Schultz and Senske (1995) have shown that the bulged topography of the plateaus surrounding the central and eastern parts of Valles Marineris can be explained by footwall uplift through trough unloading. This mechanism may have also played a role westward, but cannot explain the entire Valles Marineris topographic uplift. The interpretation by Schultz and Senske is supported by the observation that the plateaus near the cornices of the Valles Marineris grabens often display continuous bright edges about 10 km wide on images whose sun azimuth is perpendicular to the graben trend (such as orbits 64A, 65A, and 66A). They are sometimes associated with dark wind streaks. Wind is an efficient erosional process on Mars, as shown by, e.g. Ward (1979) and Greeley and Iversen (1985). The bright belt could correspond to more intense wind abrasion on the plateau edges than in other plateau parts.

On Earth, passive margins of the Gondwana continents are affected by permanent shouldering characterized by 1–5 km uplift gently attenuating several hundred kilometres away from the ocean (Weissel and Karner, 1989). The slope is the highest near the grabens, and decreases away from it to about 1 . Assuming a 30 km thick crust and

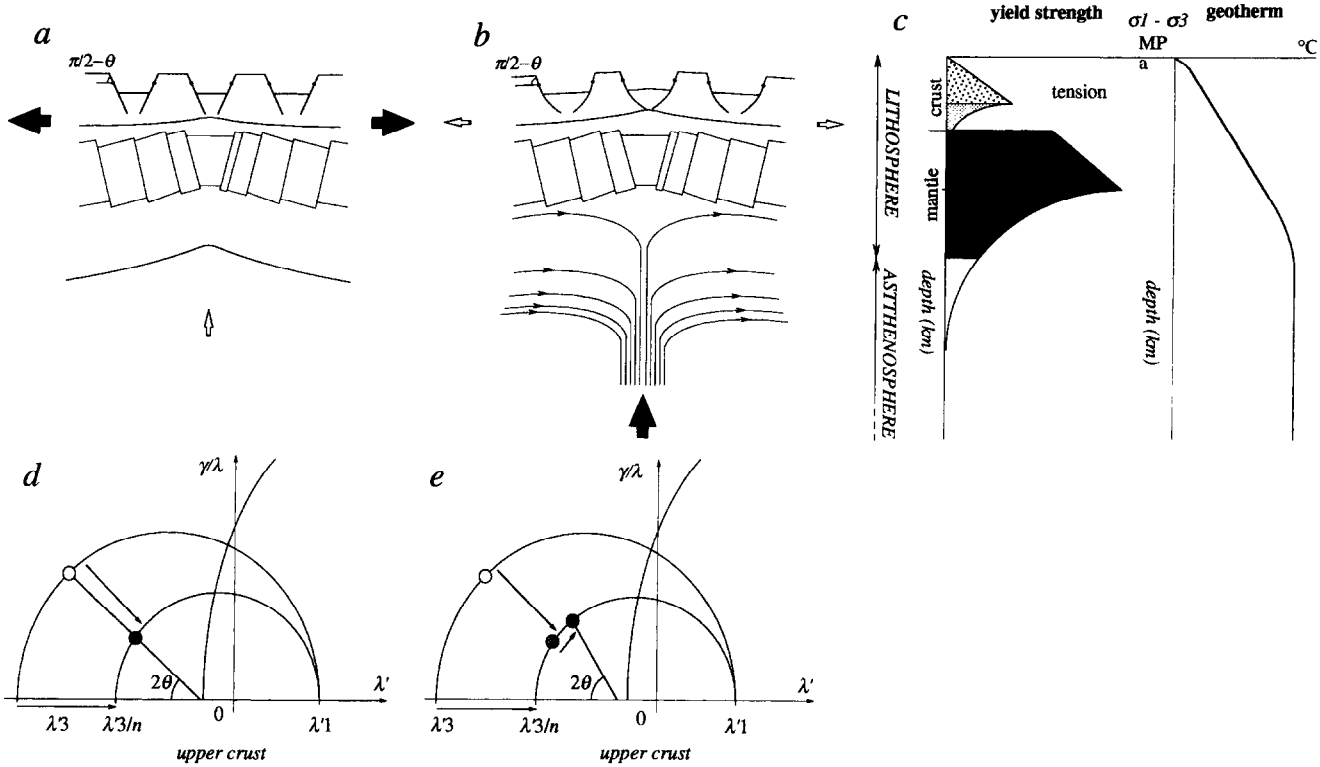

Fig. 4. Sketches explaining why block rotations may be accommodated following Brun and Choukroune's method for "domino" geometry in the case of stretching produced by mantle upwelling (b) and with more difficulty in the case of horizontal traction (a). In the latter case, strain must be distributed among several major faults with comparable vertical offsets (several kilometres), with as many synthetic and antithetic normal faults to fit observations. Rotation on synthetic faults is counteracted by rotation on antithetic faults because all are in the same strain field. Fault rotations induced by passive asthenospheric rise is assumed to be negligible in the upper crust because of the weak β value in the Valles Marineris case. If extensional forces originate from below (b), strain is distributed in the whole region on faults working independently. Rotation may occur. The black arrows indicate the driving forces and the light ones induced displacements. In (b) are shown flow lines of mantle upwelling supporting the Valles Marineris stretching. (c) Beside the cross-sections are suggested a tensile strength envelope and a geothermal profile at the time of Valles Marineris formation. The evolution of fault deformations may be represented by strain Mohr circles. The strain circles are justified here because the strain ellipsoid for each deformed object is expected to be representative of the strain ellipsoid for the whole deformed region. The circle shows reciprocal quadratic elongation λ' on the x-axis and shear strain γ divided by λ' on the y-axis. $\gamma = \tan(\psi)$, with ψ the angular shear strain. (d), (e) show the Mohr circle for the entire stretched part of the Valles Marineris upper crust, defined by $\lambda'1$ and $\lambda'3$. The influence of both mechanisms on this circle is shown. The small circles correspond to the strain expressed on each fault. In (d), for each fault the diameter of the initial strain circle is theoretically less by a factor n, which is equal to the number of faults in the case of faults with exactly the same characteristics (but opposite dip angle for antithetic faults). The white dot on the Mohr circle shows the strain if the deformation was virtually accommodated by one single fault, and the black dot shows the deformation in the case of n faults, and corresponds to the dots drawn on the fault planes. In (e) the two strain circles have the same significance as previously. The white dot corresponds to the virtual initial strain if there were one single fault, the grey dot shows the initial strain on each fault, and the black dot shows any further deformation stage on each fault. Contrary to (d), the arrow in the small circle shows that the faults can rotate contemporaneously

several kilometres of downthrown movements for these terrestrial uplifts, passive margin uplifts might correspond to the conditions prevailing during the Valles Marineris formation, 2 or 3 b.y. ago, when the Valles Marineris crust and lithosphere were thinner (e.g. Schubert *et al.*, 1992) than currently (the current elastic lithosphere and crust thicknesses being generally estimated to 100–300 and 40–70 km, respectively (Sleep and Phillips, 1985; Banerdt *et al.*, 1982, 1992)). Therefore the erosional patterns on the cornices could be due to erosion of uplifted plateau edges. The mechanism of uplift may be due to stretching rotation, however the contribution of trough unloading appears to be also necessary because the bright belts follow the spur and gully walls (most of them are assumed to represent eroded fault scarps, (Peulvast *et al.*, 1996)) as well as the landslide walls. The uplifted parts of the cornices above the border faults would have been destroyed by landsliding if the uplift were only due to stretching rotation, or to other styles of the lithospheric response to thinning.

2.4.3. *Maximum tilting angle.* In many cases of upper crustal stretching, faults lock up after a little extension and some block tilting, and then tectonic stretchings occur on a newly created fault (Jackson and McKenzie, 1983; Buck, 1993). This occurs in thick brittle lithosphere undergoing quite weak heat flux, in contrast with metamorphic core complex regions with high heat flux and thin lithosphere. Thus, if the Valles Marineris border faults rotated, it is likely that a maximum allowed rotation angle existed on each fault.

The maximum amount of rotation corresponds to the maximum possible angle between the fault plane and the maximal stress direction to keep the fault active. More precisely, according to Nur *et al.* (1986), the threshold beyond which a fault is abandoned and a new fault forms may be written as a function of the difference between the cohesive strength of the unfractured rock S_0 and the cohesive strength of pre-existing faults S_1, the coefficient of friction μ, and the effective normal stress σ_0 acting on the faults (actual regional normal stress less pore pressure).

If $\Delta\theta$ is the tilting angle, defined by

$$\Delta\theta = \alpha_i - \alpha_f \tag{1}$$

where α_i is the initial fault dip and α_f the final fault dip, this threshold corresponds to the following amount of rotation $\Delta\theta_{MAX}$:

$$\Delta\theta_{MAX} = \frac{1}{2}\cos^{-1}\left[1 - \frac{(1 - S_1/S_0)}{(1 + \mu\sigma_0/S_0)}\right]. \tag{2}$$

Rotation is related to the stretching factor, β (McKenzie, 1978), measured at the surface. Both geometrical relationships and field studies on Earth, especially in the Basin and Range (Brun and Choukroune, 1983; Angelier and Coletta, 1983; Angelier *et al.*, 1986) allow to link the dip angles after rotation with the stretching factor (Fig. 3), using the relation

$$\beta = \frac{L_f}{L_i} = \frac{\sin\alpha_i}{\sin\alpha_f} \tag{3}$$

where L_f is the final length of the stretched crust, L_i its initial length, α_i the initial dip, and α_f the final dip. β varies from 1 (stretching null) to infinity. For instance, $\beta = 1.5$ and 2.3 means that the crust has been 50% and 130% stretched, respectively. An important result concerning the β behaviour is summarized by Brun and Choukroune (1983): "rapid variations (significant) of fault dip occur during the early 50% stretching", and "fault with initial dip ranging from 90° to 50° (i.e. a 40° fan) gives at 100% stretching a 7° fan". Fault dips follow an exponential-type decrease law.

Replacing β in equation (1), the amount of rotation is linked with the stretching factor

$$\beta = \frac{\sin\alpha_i}{\sin(\alpha_i - \Delta\theta)} \tag{4}$$

and, substituting $\Delta\theta$ of equation (2) in equation (4)

$$\beta_{MAX} = \frac{\sin\alpha_i}{\sin\left[\alpha_i - \frac{1}{2}\cos^{-1}\left(1 - \frac{(1 - S_1/S_0)}{(1 + \mu\sigma_0/S_0)}\right)\right]} \tag{5}$$

where β_{MAX} is the maximum stretching accommodated by a fault before locking. According to Angelier and Coletta (1983) and Angelier *et al.* (1986), initial rift geometry locks up between $\beta_{MAX} = 1.5$ and 2, and vertical tension gashes formed during previous stages begin to move as second-order normal faults.

If the Valles Marineris faults rotated, some faults may have been locked because the amount of rotation was too high. Equation (2) may be used to define the maximum tilting angle beyond which new faults are likely to develop. On Earth the most common values have been found within the range 20°–45° (Nur *et al.*, 1986). In Valles Marineris it is difficult to define what is the depth of maximum fault rotation, however taking some realistic parameters may provide an insight on possible $\Delta\theta_{MAX}$.

Most of the border faults should probably be more than 10 km deep, and without further information, this depth can be assumed to correspond to a depth where significant rotation could have taken place. Considering a mean 3×10^3 kg m^{-3} density for the brittle crust and the 3.71 m s^{-2} value for the acceleration of gravity, the normal Martian lithostatic pressure gradient is about 11.1 MPa km^{-1}. At the beginning of the trough evolution, the lithostatic pressure would have been about 110 MPa at 10 km depth. However, due to the possible existence of groundwater and ground ice, this value may have been reduced to some 50 MPa, in the case of saturated bedrock (see p. 24 of Price and Cosgrove (1990)). Laboratory experiments of quasi-static fault growth in granite carried out by Lockner *et al.* (1991) using a process which allows a constant rate of acoustic emission to be maintained allow to hypothesize that creep in a granitic-like crust occurs at pressures of the order of 500 MPa, so that both the two boundary values for σ_0, 110 and 50 MPa, fall without doubt within the brittle domain of the Martian crust.

According to Nur *et al.* (1986), S_0 ranges from 40 to 400 MPa, according to rock hardness. The Martian basement at 10 km depth could correspond to a value on the order of 100–300 MPa. According to Nur *et al.*, S_1 is the most likely in the range 0–$S_0/2$, and is a function of fault hardening due to mineral crystallizations. The coefficient of friction μ for a granitic crust is in the range 0.5 0.7 (see p. 90 of Paterson (1978)), and 0.6 is a good mean value (Byerlee, 1978).

Figure 5 shows the maximum tilting angle corresponding to these values, inferred from equation (2). Extension modelling with block tilting presented hereafter does not take formation of new faults due to locking of previous ones into account, and thus the results of this study will have to be checked by the maximum tilting and stretching values in Fig. 5.

2.5. *Lithosphere rheology beneath Valles Marineris*

The structural layering of the lithosphere under Valles Marineris and the style of rifting are closely related. In

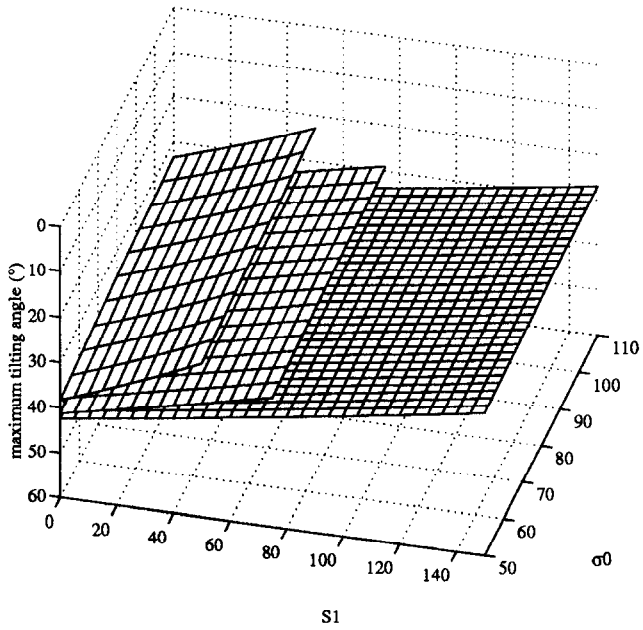

Fig. 5. Maximum angle of fault rotation for Valles Marineris under assumptions discussed in the text. The upper, middle, and lower surfaces correspond to cohesive strength of unfractured rock S_0 of 300, 200, and 100 MPa, respectively. S_1 (MPa) is the cohesive strength of the fault and σ_0 (MPa) the effective normal stress acting on the fault

the previous part of this paper we implicitly assumed that the Valles Marineris lithosphere has the same structure as the one beneath the terrestrial continental rifts. The following reasons explain why this assumption is valid.

Three modes of continental extension were defined on Earth: narrow rifts, wide rifts, and core complexes (Buck, 1991). According to Buck, the difference between these modes mainly depends on two initial conditions: the initial thermal state and the crustal thickness. Extension rate plays a role as well, but is expected to be minor with respect to the role of the initial conditions. Anderson and Grimm (1994) applied the methodology of Buck (1991) to Valles Marineris. The core complex mode for Valles Marineris is excluded from obvious image observation. Anderson and Grimm use this as a constraint for the heat flow and crustal thickness during its formation. They concluded that considering Valles Marineris as a narrow rift in a 40–60 km thick crust is in agreement with a wide range of parameters; the wide rift hypothesis is not ruled out but requires extension rates less than 1 mm y^{-1}.

According to Buck (1991), narrow rifts correspond to extension concentrated on a small area in the crust and upper mantle, and wide rifts are characterized by a uniform extension of the crust and upper mantle over an area larger than the lithospheric thickness. The widest Valles Marineris profile, across Melas, Candor, Ophir and Hebes chasmata, is 600 km long, and 400 km appears to be considered by all the geophysicists as the current extreme upper value of lithospheric thickness (Banerdt *et al.*, 1992). It is expected to be less in the past (e.g. Solomon and Chaiken, 1976; Toksöz and Hsui, 1978; Schubert *et al.*, 1992), so that strictly speaking, from this point of view, the middle part of Valles Marineris could be considered as a wide rift. The upper bound for extension rate to get a wide rift according to Anderson and Grimm (1994) does not cause timing problems, as shown by the results obtained in Section 4. The outer parts of Valles Marineris would be considered as part of aborted wide rift segments (Anderson and Grimm, 1995). Kiefer and Johnson (1995) argue in favour of a primary narrow rift structure, in which high strain rate would have led to deformations more distributed than in usual narrow rifts.

The lithospheric structure beneath wide rifts, according to Buck (1991), is made of, from top to bottom, a brittle upper crust, a thick ductile lower crust, a brittle mantle layer, and a ductile one. Beneath narrow rifts the lithospheric structure is about the same, but the heat flow is weaker and essentially leads to a more brittle behaviour in the previous brittle layers and a less ductile behaviour in the ductile layers. The upper crust is thicker and the lower crust thinner. Allemand *et al.* (1989) and Allemand and Brun (1991) studied scaled analogical modelling of rifting. They succeeded in modelling a wide rift composed of several parallel grabens in the only case of four lithospheric layers. Two layers (one brittle and one ductile) and three layers (one brittle above, one ductile below, and one more ductile at the bottom) were only able to form one or two parallel grabens (Allemand and Brun, 1991). A further constraint to get several parallel grabens is a strong decoupling at the crust/mantle boundary. The number of grabens is proportional to the degree of coupling.

Allemand *et al.* (1989) obtained four slightly asymmetric grabens with the four layer hypothesis and a strong crust/mantle decoupling. Although the precise number of grabens may not be essential, one can compare this result with the geometric configuration of the widest Valles Marineris profile, which includes Melas, Candor, Ophir, and Hebes chasmata. Although this profile was intensively eroded since the main tectonic episodes, the grabens of the adjacent profiles are also slightly asymmetric (Schultz, 1991; Mège, 1991; Mège and Masson, 1994a).

Figure 4 shows the lithospheric structure adopted in our model of Valles Marineris as a function of the arguments discussed below. Figure 4c indicates the corresponding rheologic profile. Four lithospheric layers are taken into account above the weak asthenosphere.

Footwall uplift due to necking is expected if a ductile crust exists, and is independent of the occurrence of the shear mechanism of thinning, as illustrated in the study by van der Beek *et al.* (1994). Whereas Kusznir *et al.* (1991) investigated simple shear in the brittle crust, Lin and Parmentier (1990) numerically modelled footwall uplift in an entirely purely (and symmetrically) stretched graben, which might provide an interesting analogy with the Valles Marineris case. Since necking is a permanent support, footwall uplift should be observed in Valles Marineris if a ductile crust existed when it formed. Even if the lithosphere cooled enough to be entirely brittle now, the shoulders produced this way (i.e. mechanically, not thermally) should be fossilized.

3. Method

Two simple methods to calculate stretching factors were used. The first one assumes that block tilting is null or

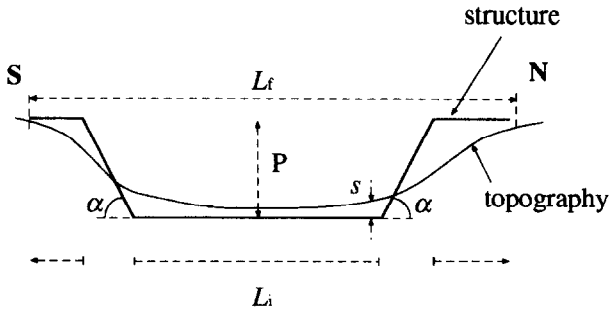

Fig. 6. Definition of the parameters used in calculations, in the simplest, single graben case

negligible and the second one considers that it plays a significant role. They were applied in a first stage to Ius Chasma (independently from the other troughs) and then to the entire Valles Marineris graben system.

The parameters to be fixed for calculation of β are: α, fault dips, P, vertical offsets, L_f, the current profile lengths across the considered graben, and L_i, the initial profile length (Fig. 6). The cross-sections and minimum vertical fault throws (plateau elevation less floor elevation) (Figs 7 and 8) were established from the Digital Elevation Model of Mars computed by USGS (1992). The height accuracy of the DEM is ± 1 km, and its lateral resolution is a few kilometres. This uncertainty should not alter the validity of the results because the other parameters, such as sediment thickness and fault dip, were varied in order to cover a wide range of geometric configurations. The low vertical and horizontal DEM resolution are thus implicitly accounted for. For profiles D and E, the USGS DEM can be compared with the DEM of Ius and Tithonium Chasma established at University College London (Fig. 9) (Day *et al.*, 1992; Muller *et al.*, 1993). The USGS DEM was derived from digitized contour maps, and some of the steps for DEM generation were manually carried out. Conversely, the UCL DEM has been derived from automated digital matching of image stereo-pairs, improving both the lateral DEM resolution and height accuracy (a few hundred metres). Both techniques are very different, and give an idea on the reliability of the profiles. The discrepancy between the UCL and USGS DEMs is almost everywhere less than 1 km. The comparison of both shows that if the UCL DEM is better than the USGS DEM, then the fault throws could be often higher (0.5–1 km) than usually estimated. Future DEMs in Valles Marineris resulting from digital matching of stereo-pairs are needed to transform many speculations on Valles Marineris topography and structure into certainties.

The faults observed at the surface may represent part of the structures existing in Valles Marineris only, some other ones being possibly buried. The results will thus provide minimum stretching estimations.

Profile lengths have to include the whole width of the extended area at its widest profile (Fig. 7). We chose $L_f = 110$ km for Ius Chasma and $L_f = 660$ km when the entire Valles Marineris is considered. The structure of Tithonium Chasma is unclear. On several sites displaying evidence of recent faulting, Tithonium Chasma may have a graben structure. However this may not be the case in the entire trough (Mège, 1991; Peulvast *et al.*, 1995) and both end-member cases were considered: (1) a graben-type structure; (2) no tectonic extension.

3.1. *Extension without block tilting*

3.1.1. *Input parameters. Dip angles α_1 and α_2.* Planar faults and dips within the range of 40°–80° are assumed. We do not take the 90° case into account because theoretically it would imply an infinite subsidence. This case will be considered when tilting will also be considered.

We modelled stretching for both identical and different fault dips, α_1 and α_2, on each graben of each profile. The case of asymmetric fault dip is investigated: in a simple graben, the two border faults have different dips ranging between 40 and 80° each. On profiles B and F two border faults are assumed to have the same dip, and the two other ones, another but identical dip.

Vertical offsets P_1 and P_2. Vertical offsets include both the whole wall heights and sediment thicknesses. Very poor information exists on the amount of sediments on the Valles Marineris floor. It cannot be compared with the quantity of bedded sediments (Nedell, 1987) because the latter appear to have formed after the development of the spur and gully morphology, which is contemporaneous to most of the graben formation (Witbeck *et al.*, 1991; Peulvast *et al.*, 1996).

Sedimentary deposits in Coprates Chasma are probably thin (Schultz, 1991), since some remnants of large diameter craters, expected to have been carved into plateau materials, are observed on canyon floors. We attempted to infer the depth of the buried plateau underneath two such craters, located on the Coprates and Ius Chasma floors, respectively (A, B on Fig. 2).

For craters less than 21 km in diameter (p. 133 of Melosh (1989)), the theoretical rim height is equal to $h = 0.036D^{1.014}$ (Pike, 1977). The rim height of the first crater, 15 km in diameter, should have been about 560 m before erosion. The diameter of the second crater is about 7.7 km and its rim height should have been about 285 m. The current rim heights for both cannot be precisely defined from the available topographic information; however, the most important thing is that they can still be observed. If they directly formed on plateau material, the sedimentary blanket should be very thin, a few hundred metres at most. These craters may also have formed later, but they appear to be highly degraded and must be quite old anyway, implying a rather thin blanket as well.

From this information we assume that the sediment thickness in Valles Marineris may range from very few (0 km as an end-member value) to 1, 2 or 3 km at most. We assume that all the current elevation of the plateau is due to tectonic subsidence of the canyon floor. This seems plausible since faceted spurs often reach a very high level on the wallslopes. The vertical throws recorded on present walls do not exceed about 10 km (USGS, 1991): this implies that the maximum possible vertical offsets are likely to be around 13 km. This assumption of a bulk 3 km value for the maximum sediment thickness allows to take into account possible local variations, like unsuspected very high sediment thicknesses in Melas Chasma for

instance. Because of the complexity of its (essentially buried) structural, and geomorphological histories, the structure of Melas Chasma is mostly unconstrained. Sediment thicknesses might be higher than in other parts of the trough system. The flexibility of the model fits with the assumption of 5 km sediments in Melas Chasma, together with more than 2 km in both Candor and Ophir chasmata, as well as the assumption of 3 km in the three troughs.

In Ius Chasma, we assume that Geryon Montes are a horst but did not significantly subside tectonically, at least from its eastern end up to the longitude of profile B. On profile B its elevation is more than 7 km above the canyon floor (USGS, 1986) and the adjacent plateau elevation is 8 km. The lacking 1 km can be reasonably attributed to erosion during the 2 or 3 b.y. long-lasting Geryon Montes evolution (Neukum and Wise, 1976; Hartmann *et al.*, 1981).

The elevation of the Geryon Montes crest diminishes eastward from profile B (USGS, 1986) and Geryon Montes finally disappears under the canyon sedimentary cover near longitude 78°W. On profile C we expect that Geryon Montes might still be present under the sediments s, the thickness of which has been assumed to be 3 km at most. We consider in computations that vertical offsets P on both sides of Geryon Montes range between 0 and $s-0.5$ km.

3.1.2. *Calculation.* The strectching factor is deduced using equation (3), which may be precised according to the parameters defined on Fig. 6:

$$\beta_{NR} = \frac{L_f}{L_f - \sum_1^n \frac{P_{(n)}}{\tan \alpha_{(n)}}} \tag{6}$$

where β_{NR} is the stretching factor in the non-rotational case, and n is the number of border faults.

3.2. *Extension with block tilting*

3.2.1. *Input parameters.* We use in this method the same parameters as in the previous one. The 110 km value for the final length L_f and the hypotheses on the vertical offset P are kept. We take 60° and 90° as initial dip angle values

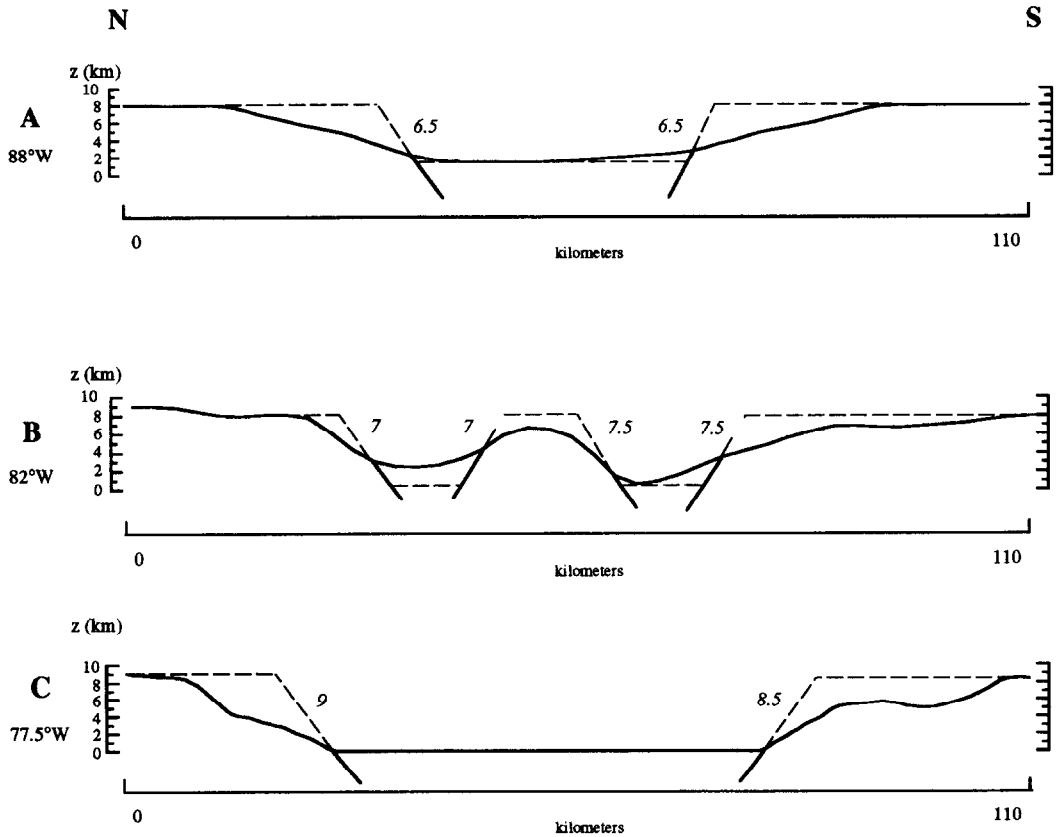

Fig. 8. Topographic profiles across Valles Marineris (location on Fig. 7), and structural interpretations. As a lower boundary condition, no sediment thicknesses, except those corresponding to the stratified deposits, are represented. In models we assume higher boundary conditions corresponding to a bulk 3 km sediment thickness in all the canyons. On any profile of Fig. 7, more sediments in one canyon are compensated by less sediments in the others. This figure is mainly derived from observation of high resolution pictures, topographic maps (USGS, 1980, 1986), digital topographic maps at 1/16° at 1/64° per pixel (USGS, 1992), and works by Nedell (1987), Peulvast *et al.* (1995), and Mège and Masson (1994b). Numbers are estimations of the minimum vertical offsets of border faults in kilometres (sedimentary thicknesses other than those of layered formations have to be added to these values). These numbers are used to calculate the stretching factor with the non-rotational and the rotational methods. For each value, the cases with sediment thicknesses between 0 and 3 km were considered. The dip angles on the figure are arbitrary

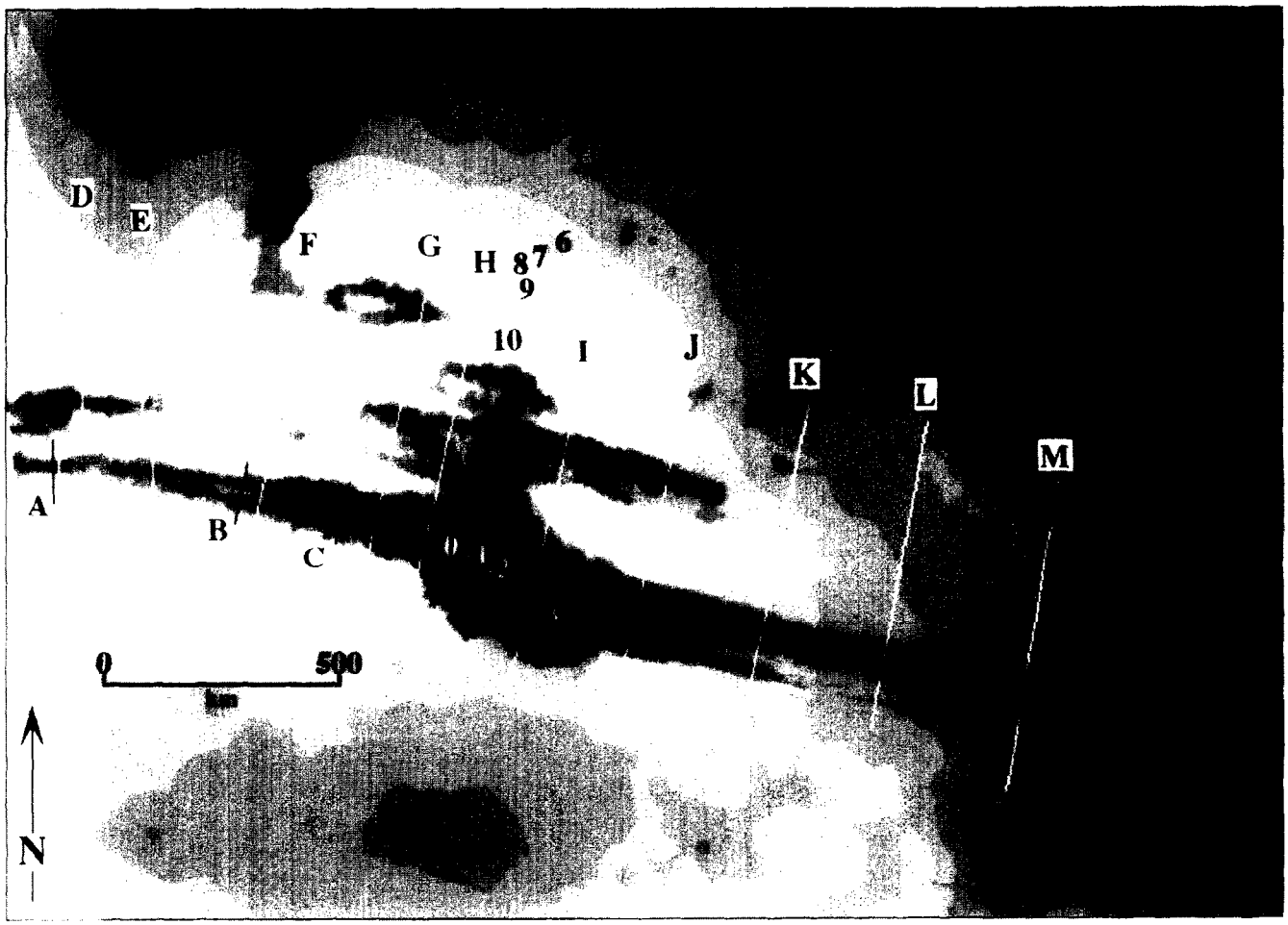

Fig. 7. Topographic map of Valles Marineris and location of topographic profiles used for calculation of stretching (cross-sections displayed and interpreted on Fig. 8). Numbers refer to contours (km) (USGS, 1992)

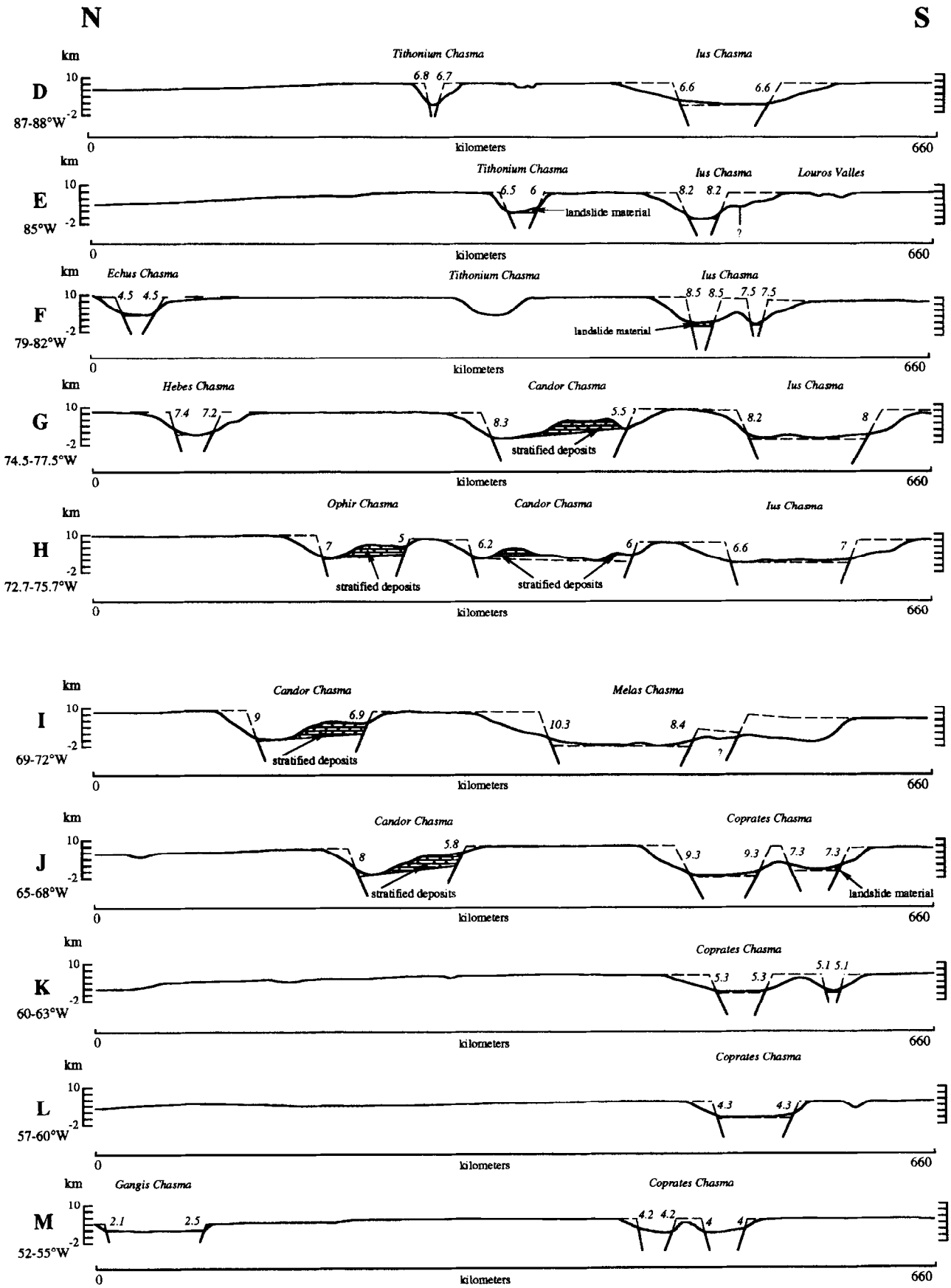

Fig. 8. (*Continued*)

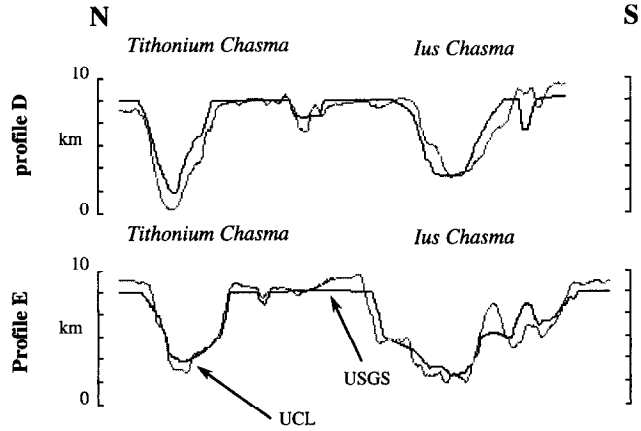

Fig. 9. Comparison of topographic profiles D and E (Fig. 7) given by USGS and UCL DEMs (USGS, 1992; UCL, unpublished, used with permission)

α_0. Significant tilting for smaller initial angle values, such as the 40° case investigated in the non-rotational case, are obtained for very high stretching factors only (Fig. 3) unexpected in Valles Marineris, so that such low angles are not considered here.

3.2.2. *Calculation.* Modifying equation (6), the stretching factor is given by:

$$\beta_R = \frac{\sin\left[\tan^{-1}\left(\frac{P}{L_f - L_i}\right)\right]}{\sin\left[\tan^{-1}\left(\frac{P}{L_f - L_i}\right) - \Delta\theta\right]}. \quad (7)$$

The calculations have been proceeded following interactive iterations, assuming a globally synchronous stretching mechanism for each graben. In this process, the evolution of α, θ and s may be visualized at any intermediate deepening stage. However the results presented here, to make the interpretations clearer, consider the initial stage (no sediments) and the maximum reasonable stage (3 km thick sediments).

The whole method is described in Mège (1994), and does not need to be discussed much here. We consider that the rotational process may be approximated by discrete successive stretching stages during which small amounts of rotation are completed. The grabens are "closed" with successive decrementation steps from their current geometry to the initial horizontal profile. During the iterations, the variations of α and P are recorded, and the iterations stop when P reached the value required to account for the quantity of sediments desired on the graben floor. Then the initial and final values of α are compared in order to find $\Delta\theta$.

4. Results

The along-strike variations of stretching in both rotational and no rotational cases are the same, but under similar conditions rotation increases the amount of stretching. For instance, 60° initial dips in the rotational modelling of Ius Chasma would lead to 30 km stretching with $s = 0$ on the small B profile, versus 59 km with $s = 3$ km. In the non-rotational case, these conditions would respectively lead to 20 and 30 km stretching (Fig. 11). At the Valles Marineris scale, block tilting on the longer J profile would lead to 31 and 45 km stretching with $s = 0$ and 3 km, respectively; these values would decrease to 28 and 40 km without tilting (Fig. 13a).

The latter examples refer to the most stretched profiles. They illustrate the fact that rotation or non-rotation has a significant influence on the ratio between the width of the deformed zone (canyons) and the width of the undeformed zone (roughly the plateaus). When a small plateau length is considered, tilting is responsible for an important stretching increase. For the Ius Chasma profiles, the stretching increase reaches 50% in the previous example. On profiles taking into account more undeformed plateau zones, stretching is lower. For the Valles Marineris profiles the stretching increase due to rotation is a few kilometres at most (10% of additional stretching). To summarize, when tilting is considered, the choice of the dimensions of the geodynamic unit, and thus the profile length, including both areas where deformation concentrated and non-deformed areas, has direct implications on the amount of tilting and fault flattening in the results.

4.1. *Ius Chasma (Figs 10 and 11)*

The stretching factors are shown on Fig. 10 (asymmetric configurations) and Fig. 11 (symmetric configurations). β is generally moderate, even with 3 km thick sediments on floors between 80° and 60° dip angles. In these conditions, under the non-rotational configuration (Figs 10 and 11a, b), β is in the range 1.02–1.11 (2.2–12.1 km) at 88°, 1.05–1.27 (5.5–30 km) at 82°W, and 1.03–1.18 (3.3–20 km) at 77.5°W for a 100 km final profile length, corresponding to about the distance between the northern and southern slopes of Ius Chasma on profile C. The maximum stretching is reached by the 40° dipping configuration calculated with 3 km sediments, and leads to $\beta = 1.8$ (profile B on Fig. 10, and Fig. 11a). β rapidly falls down to 1.2 when both faults have a dip $\leqslant 60°$ (Fig. 10). With $\beta = 1.8$ the profile length before stretching would have been about 60 km. However, we think that four initially 40° dipping faults is an unlikely configuration. Despite important error bars due to uncertainty on sediment thicknesses and distribution, these variations clearly indicate an increase of extension eastward from the western end of Ius Chasma to 82°W. Under the rotational configuration (Fig. 11c, d), the variations of stretching are similar but the higher and lower stretching values for initial 60° and 90° dipping faults are 1.1 and 59 km.

The maximum stretching in terrestrial continental rifts is observed in the central part of rifts. Thus if Valles Marineris can be compared with terrestrial continental rifts, stretching is expected to increase eastward in Ius Chasma up to the centre of Melas Chasma. However, β decreases east of profile B. This is due to the absence of Geryon Montes in the eastern part of Ius Chasma, even when a 2.5 km high Geryon Montes is assumed to exist and be buried under 0.5 km sediments east of its current

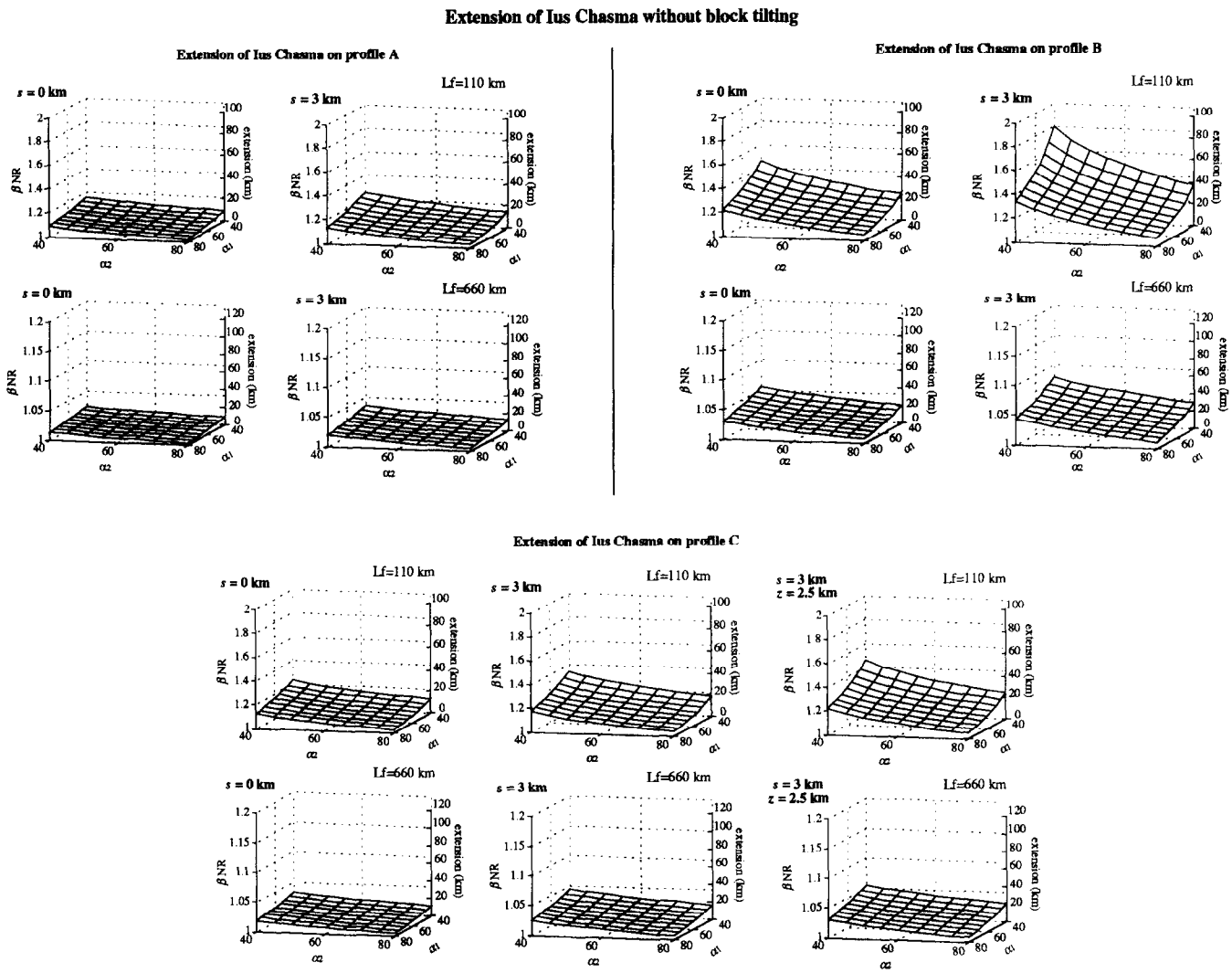

Fig. 10. Results of computation in Ius Chasma in the non-rotational cases for variable combinations of dip angles on border faults. α_1, α_2 = dip angle, s = sediment thickness. In each graben half of the faults is expected to have an α_1 dip and the other half an α_2 dip. Evolution of the stretching factor β is given as a function of α_1, α_2 and vertical offsets of border faults. On profile C a horst is expected to be buried under sediments east of the current topographic end of Geryon Montes. The horst is bounded with two border faults whose vertical offsets are equal to z = 2.5 km. Location of profiles on Fig. 7

topographic end (compare profiles B and C on Figs 10 and 11a).

This may be explained two ways. (1) It is possible that the extensional structures buried below floor sediments have a more complex geometry than expected with this model and accommodated more deformation. For instance, several shallow horst and graben structures might exist, and could be able to sufficiently increase stretching at 77°W to average or exceed the stretching factor calculated at 82°W. (2) At the 77.5°W longitude, and farther east, the canyon system strongly widens and an important amount of stretching is accommodated in the Candor, Ophir and Hebes grabens. Thus, it would not be surprising that the stretching factor measured in the Ius Chasma region is not representative of the whole Valles Marineris stretching at this longitude. Extension may decrease eastward at the Ius Chasma scale but increase at the Valles Marineris scale.

The comparison between Fig. 11b, d and Figs 13, 14 indicates that the eastward stretching lowering in Ius Chasma is indeed strongly compensated by stretching at the entire Valles Marineris scale. Considering the case for tectonic stretching in Tithonium Chasma or not does not influence the global variations of stretching.

4.2. *Valles Marineris* (*Figs 12–14*)

The variations of β are shown on Figs 12–14. Figure 12 shows that the amount of stretching is only a little dependent on the dip angle in the outermost parts of Valles Marineris (profiles D and L). An asymmetric structure very weakly influences the amount of stretching if the dips are within the range 60–80° on profiles D, E, K, and L (stretching $\leqslant$ 10 km), but for one low angle (40°) border fault and a steep second border fault, asymmetry influ-

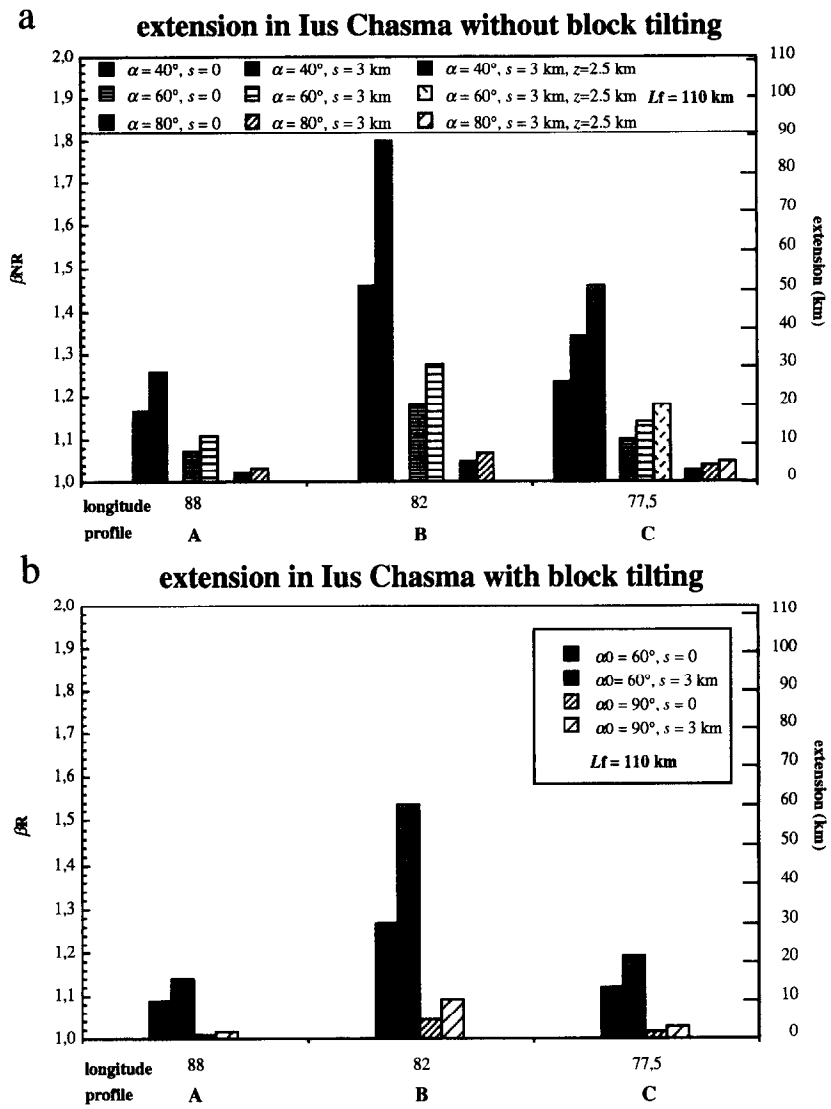

Fig. 11. Extension of Ius Chasma assuming no block tilting (a, c) and block tilting (b, d) if all the faults have the same α dip, with $\alpha = 40°$, 60°, and 80° (a, c) or the same initial α_0 dip, with $\alpha_0 = 60°$ and 90° (b, d). (a, b) profile length: 110 km; (c, d) profile length: 660 km (standardized to the profile length used for the whole Valles Marineris calculations for comparison with Figs 12–16)

ences β a lot. The sediment thickness has an appreciable influence on stretching for most profiles.

The general trend is stretching increase from Noctis Labyrinthus to central Valles Marineris, and then stretching decrease to the east; finally a small increase is recorded further east, at the far eastern part of the graben system. Unfortunately, the structural evolution of this wide chaotic area and of Gangis Chasma region during Hesperian is far from being completely understood, because of the catastrophic geomorphological events that occurred in these areas, and because of the poor resolution of pictures. The following section discusses the possible interpretation of Valles Marineris as a terrestrial continental rift as far as stretching variations are concerned. This interpretation minimizes the role of Tharsis in the Valles Marineris opening. However Tharsis-related stresses should have influenced the Valles Marineris development, and their role will also be discussed.

4.2.1. *Comparison of stretching variations along Valles Marineris and terrestrial continental rifts.* To fit the terrestrial continental rift comparison, the stretching factor β in the central area must be at least equal (as a lower boundary condition) to the stretching factor calculated in the neighbouring regions. In Valles Marineris the maximum stretching is obtained in the central troughs, close to its boundaries with Ius and Coprates chasmata. Figures 13 and 14 indicate that this maximum is expressed by two higher values, recorded on profiles G and K. An unexpected low is observed in the models in the very central regions of Valles Marineris, corresponding to profiles H and I. If Valles Marineris is a rift, this low must be an artifact, due to (1) variations of sedimentary thicknesses along the troughs; (2) existence of buried structures, or both.

Variations of sedimentary thickness. Figures 13b and 14b are linear interpolations of Figs 13a and 14a. The curves show the variations of β if the sediment thickness is constant ($s = 0$ or 3 km) along Valles Marineris, whereas the dashed intervals show what can be expected if variations of the sediment thickness exist along the

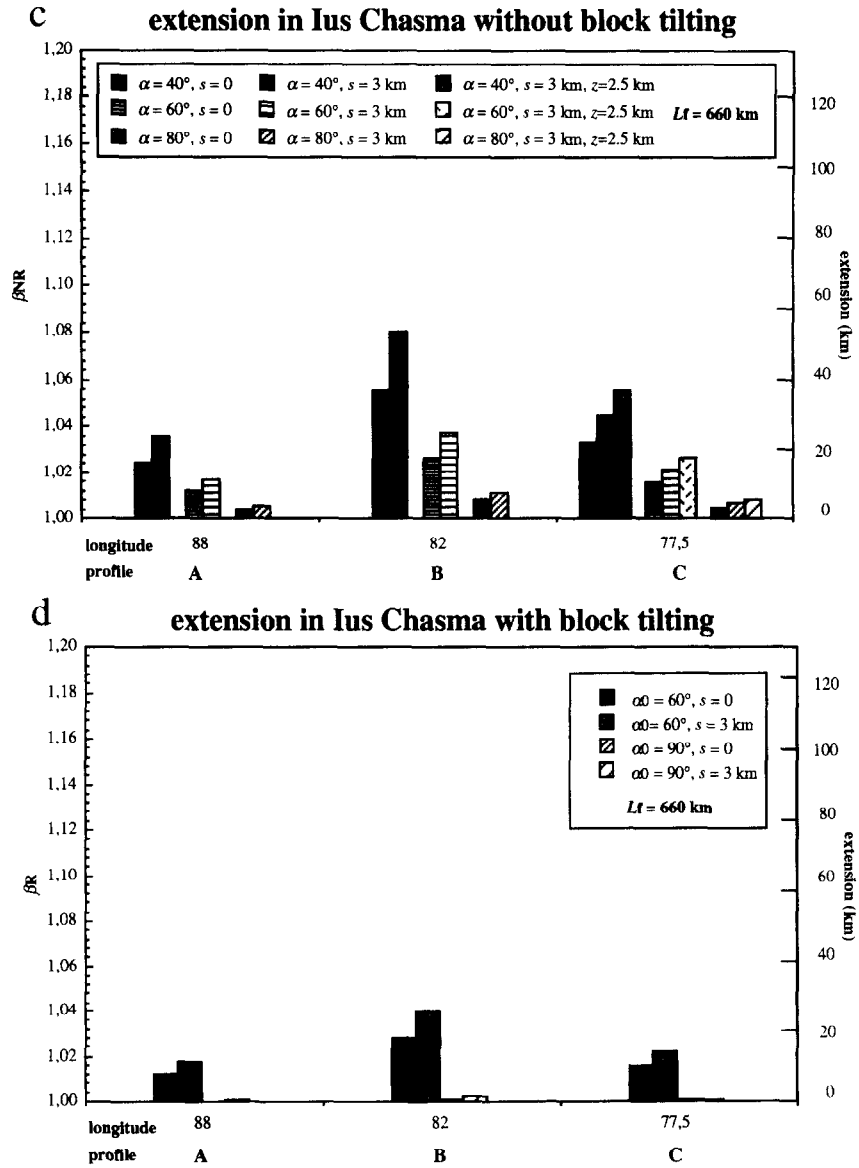

Fig. 11. (*Continued*)

grabens. The thick curve on Fig. 14b is an example of a possibly correct variation of β along the troughs, and shows that the low β in the central troughs may simply be an artifact reflecting these variations. In this example, rotations occur along initially 60° dipping faults. Stretching increases from profile D to F, where β reaches 1.044. With this value, β may remain constant up to profile J, and then decrease westward. This would imply that $s \approx 0$ km at profile F, increases to $s \approx 3$ km up to profile I, and then dramatically decreases at profile J. This feature is observed whatever the fault dips. Such a pattern of β variation does not in fact require 0 km sediments at the Melas Chasma western and eastern bounds as shown on Fig. 14b. Sediments could be 2 km thick there, merely this scheme would require that they are about 3 km thicker between. Such variations would be consistent with the suspected thicker sedimentary deposits in Melas Chasma than in the other grabens. However, in the wide range of parameter values used in the model, a very small number of possibilities allow β to remain constant.

Buried structures. Alternatively, buried structures certainly exist in Valles Marineris, some of them outcropping in the western part of Coprates Chasma (D on Fig. 2). We attempted to calculate what would be the lacking vertical throws corresponding to unobserved stretching (buried structures) in central Valles Marineris, in order for β to reach its values in the neighbouring areas (Figs 15 and 16). We investigated only the case for a 3 km thick sediment blanket, since it is likely that this region underwent intense deposition which is not currently removed. Assuming that all the deformation occurred on faults with identical dip, we found that 9 and 18 km of additional vertical offsets in the direction perpendicular to the profile trend are necessary, at the longitudes of profiles H and I, respectively, to get a constant stretching from the eastern bound of Ius Chasma to the western bound of Coprates Chasma in the case of no rotation (Fig. 15). The values obtained in the case of block rotation are 16.5 km ($\alpha_0 = 90°$) or 17.5 km ($\alpha_0 = 60°$) for profile H and 22 km ($\alpha_0 = 90°$) or 26 km ($\alpha_0 = 60°$) for profile I (Fig. 16). These additional vertical kilometres may be obtained by assuming that the deformation is distributed among

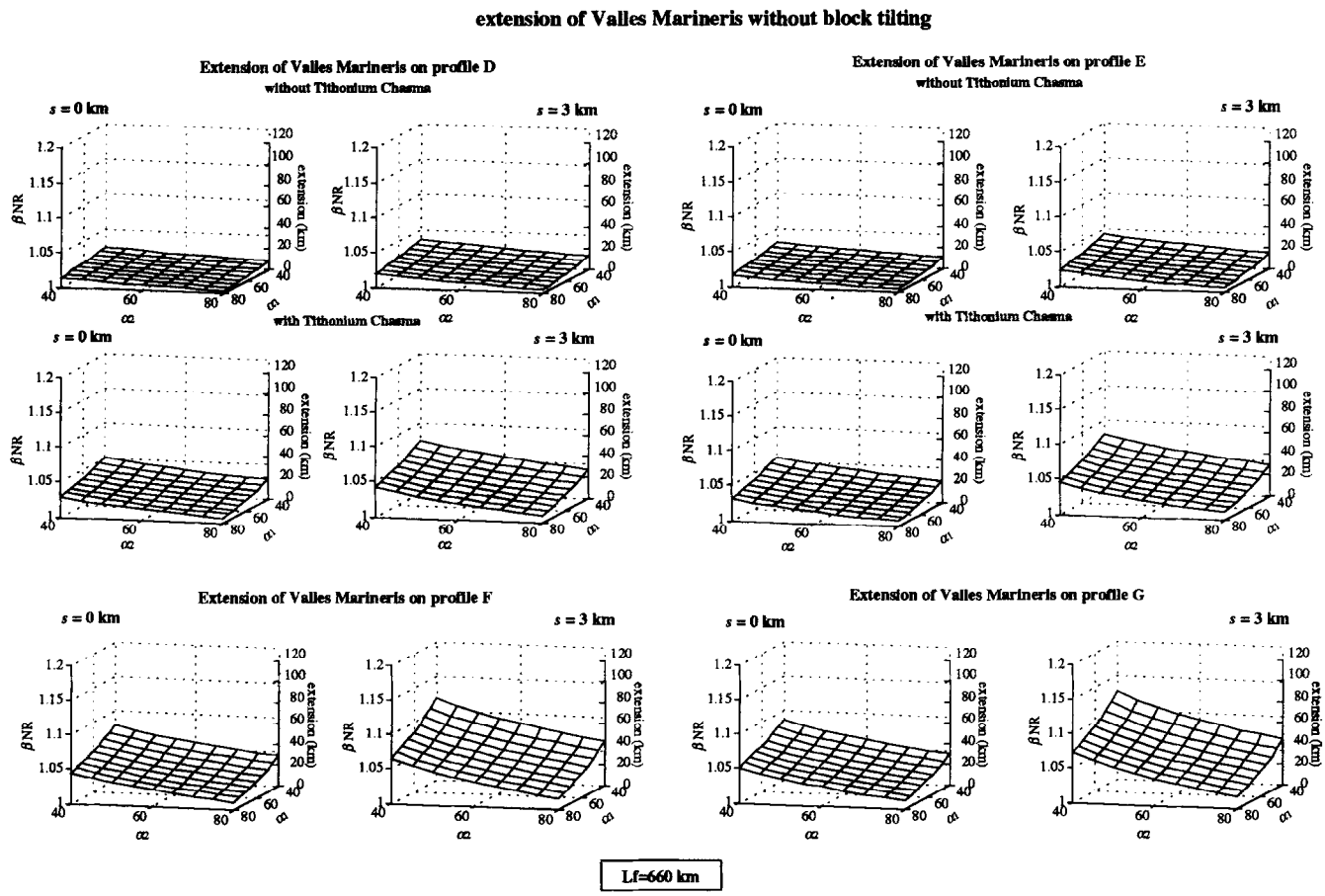

Fig. 12. Results of extension calculations in Valles Marineris in the non-rotational cases for various combinations of dip angles on border faults. Same parameters and representation as for Fig. 10. In each graben, half of the faults are assumed to be α_1 dipping and the others α_2 dipping

more faults than expected in our modelling (a few faults with major offsets or many faults with minor offsets, or a combination of both).

Variations of sedimentary thickness and buried structures. Assuming no block rotation, 1.5 km of additional floor sediments located at the bottom of each of the six major faults displayed on profile H, and masking 1.5 km of additional vertical offsets in the direction perpendicular to the profile trend, are sufficient to absorb the 9 km offsets required. If block tilting occurred, 3 km additional offsets on each fault are required. Alternatively, or in addition, a buried structure could exist in Ius Chasma on profile H, and could for instance correspond to an eastward continuation of Geryon Montes. A few structures, sometimes underlined by fissural volcanism, are observed on the Ius floor in the continuation of Geryon Montes (C on Fig. 2). Another contribution to stretching may be provided by subsidence of the portion of the plateau located between Ius and Candor chasmata. However its subsidence is particularly pronounced north of Melas Chasma, but is probably weak at the longitude of profile H. Its elevation is close to 8 km : 2 km less than the plateau north of Ophir Chasma, but not significantly less than the plateau south of Ius Chasma.

The lack of some 18 km vertical offsets on profile I in the case of no block tilting, or 22–26 km in the case of block tilting addresses a more serious problem. On profile I, the free air vertical offsets on walls belong to the highest ones in the whole trough system (more than 10 km for the north bounding fault of Melas Chasma with $s = 0$). Even with a sedimentary cover constantly 2 km thicker than on the adjacent eastward J profile, some 10–18 km high offset remains to be found. Part of the lacking extension may be absorbed by the numerous narrow grabens of Ophir Planum, studied by Schultz (1991). However there is evidence in the western part of Coprates Chasma that its structural framework is probably significantly more complicated than in our model. Some low elevation plateau remnants (D on Fig. 2) indicate that the floor structure is in fact likely more complex than what is suggested by the current topography and in our simple model. We thus suggest that buried structures exist, at least on profile I, and could be responsible for a cumulated vertical offset of 10–15 km. In addition, variations in sedimentary thickness are also likely to be included in calculations of the most realistic structural model and in further stretching calculations.

4.2.2. *Stretching increase toward Capri, Eos and Gangis Chasma.* Another important point is the significant increasing stretching trend in East Valles Marineris toward the chaotic Eos and Capri chasmata regions (Figs 13 and 14). This trend is emphasized by the presence of

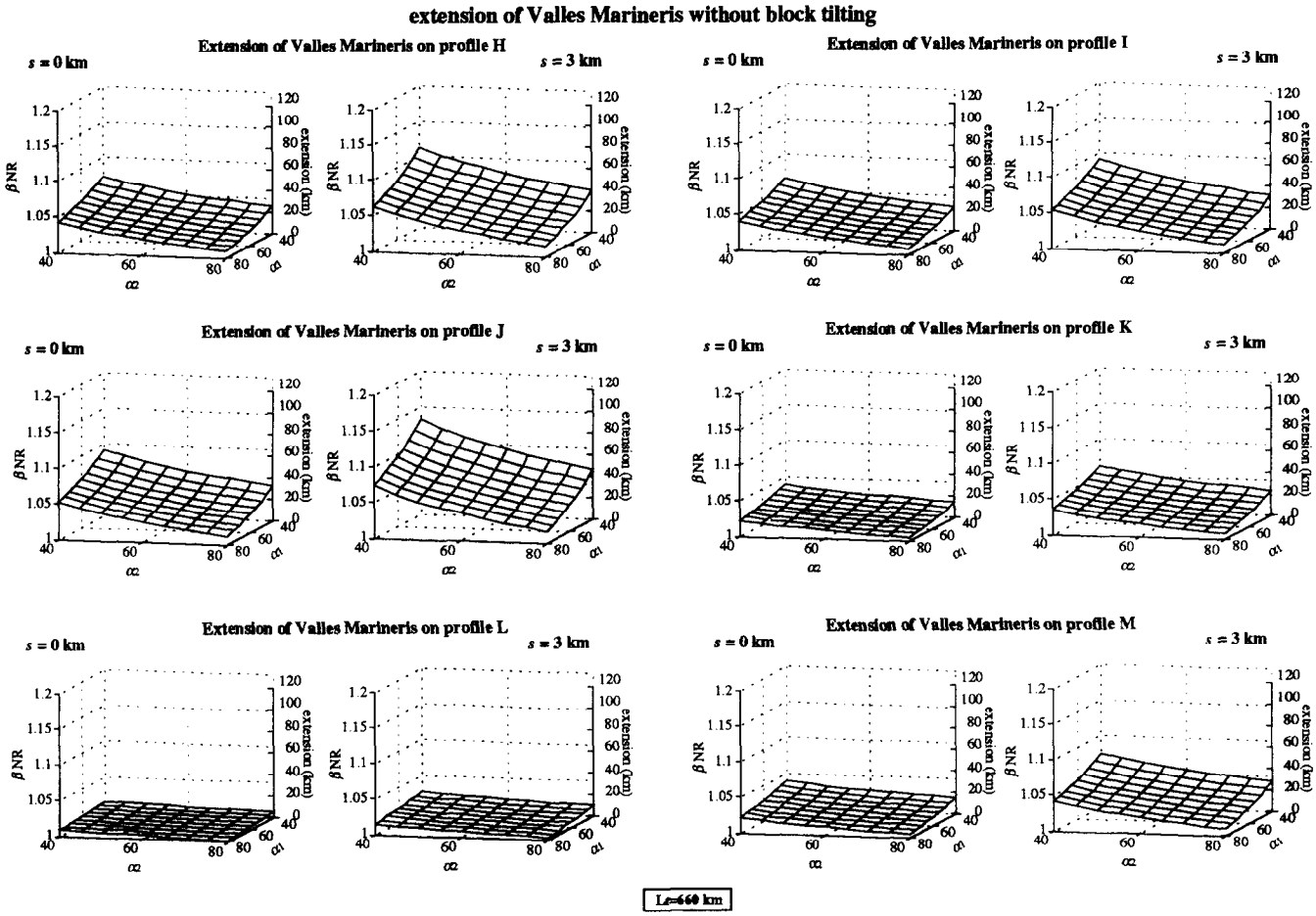

Fig. 12. (*Continued*)

Gangis Chasma northward, whose existence was included in calculations. Despite the lack of high resolution pictures, Gangis Chasma has a probable structural background on which intense geomorphological events took place. Its E–W direction is slightly different than most of the other trough trend but it seems clear that Gangis Chasma belongs to the Valles Marineris system. Its border faults are probably in the continuation of the major fault sets of the other troughs. Its E–W direction is consistent (1) with the counterclockwise evolution of the Coprates Chasma border fault trend southward; (2) with the *en échelon* trend east of Candor Chasma (E on Fig. 2); and (3) with the apparent global reorientation of structural trends in Capri Chasma toward the NE–SW direction.

The Gangis Chasma walls seem to be more than 2 km high (USGS, 1992) above the sedimentary cover. But the latitudinal division of Coprates Chasma in two parts at its eastern end would have been sufficient to observe the increasing eastward stretching displayed on Fig. 13. We suggest that the characteristics of stretching in central Valles Marineris and in East Coprates might not have been similar. Some grabens of Valles Marineris are slightly asymmetric, whereas the morphology and profiles of the eastern part of Coprates Chasma and in Gangis Chasma (profile M on Fig. 8) are surprisingly symmetric according to the currently available topographic data and morphotectonic analysis of the wall (Peulvast *et al.*, 1996). This symmetry also tends to argue in favour of different stretching mechanisms.

4.3. *Rotation angles*

The lack of flank uplift due to the lithospheric response to thinning, the diminution of dip angles due to block rotation during stretching is equal to the height of shoulders. According to our calculations, α_f is always higher than $\alpha_0 - 6^\circ$ (Fig. 17), and thus the slope of an initially horizontal plateau edge resulting from stretching is expected not to exceed a few degrees (6° in the case of a perfectly rigid crustal behaviour). The total permanent shouldering in the rotational case should thus take a maximum of 6° of stretching rotation into account, minus the possible effect of rock compaction at depth produced by the lithostatic pressure, plus an additional component of lithospheric response to thinning.

When block tilting is considered, faults may lock due to inadaptability of the sliding plane to the orientation of the least compressional remote stress (Section 2.4.3). The least favourable case investigated in Fig. 5 allows maximum tilting angles between 23° and 42°, in agreement

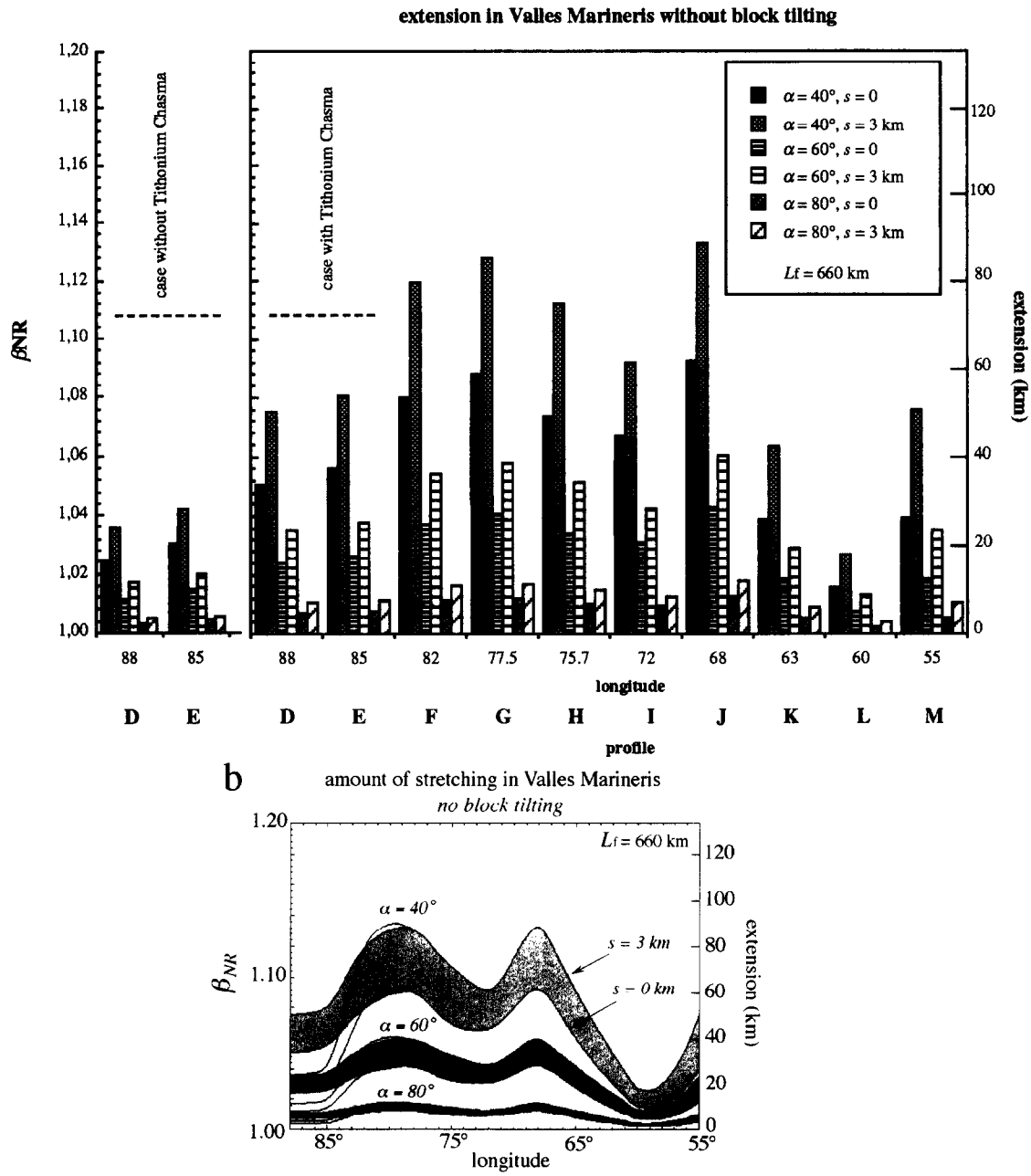

Fig. 13. (a) Extension of Valles Marineris assuming no block tilting if all the faults have the same α dip, with $\alpha = 40°$, 60°, and 80°, and with $s = 0$ and 3 km. (b) Interpolation of the results presented in (a). Tectonic extension (dashed intervals) and no tectonic extension (light intervals eastward) in Tithonium Chasma are considered

with the results shown on Fig. 17. Taking a wide range of other values for the parameters in equation (2) leads to maximum rotation angles comprised between 19° and 42°. Overall, each fault considered during calculations is mechanically able to work from the beginning of trough opening up to the end of the tectonic evolution of Valles Marineris, without the requirement for forming new faults. The faults observed within the Valles Marineris walls (Mège, 1991; Chadwick and Lucchitta, 1992; Peulvast and Masson, 1993; Peulvast *et al.*, 1996) are thus expected to be synthetic and antithetic normal faults branched with the main border faults at depth; they should reflect the influence of the free topographic boundary on development of the uppermost parts of the faults, as frequently observed on Earth in active extensional basins.

4.4. *Is there a detachment fault beneath Valles Marineris?*

All the results, including the most favourable ones, indicate that the stretching factor, usually less than 1.2, is probably too low for a detachment to develop.

This low stretching also means that if Valles Marineris were a terrestrial continental rift, it would probably not develop strongly asymmetric border faults. The small asymmetry in several grabens observed by Schultz (1991), Mège (1991) and Mège and Masson (1994a), together with the apparent symmetry of some other grabens (Peulvast *et al.*, 1996) are not absolute evidence, but strong consistencies with the architecture of terrestrial continental rifts, even if their dynamics may be different.

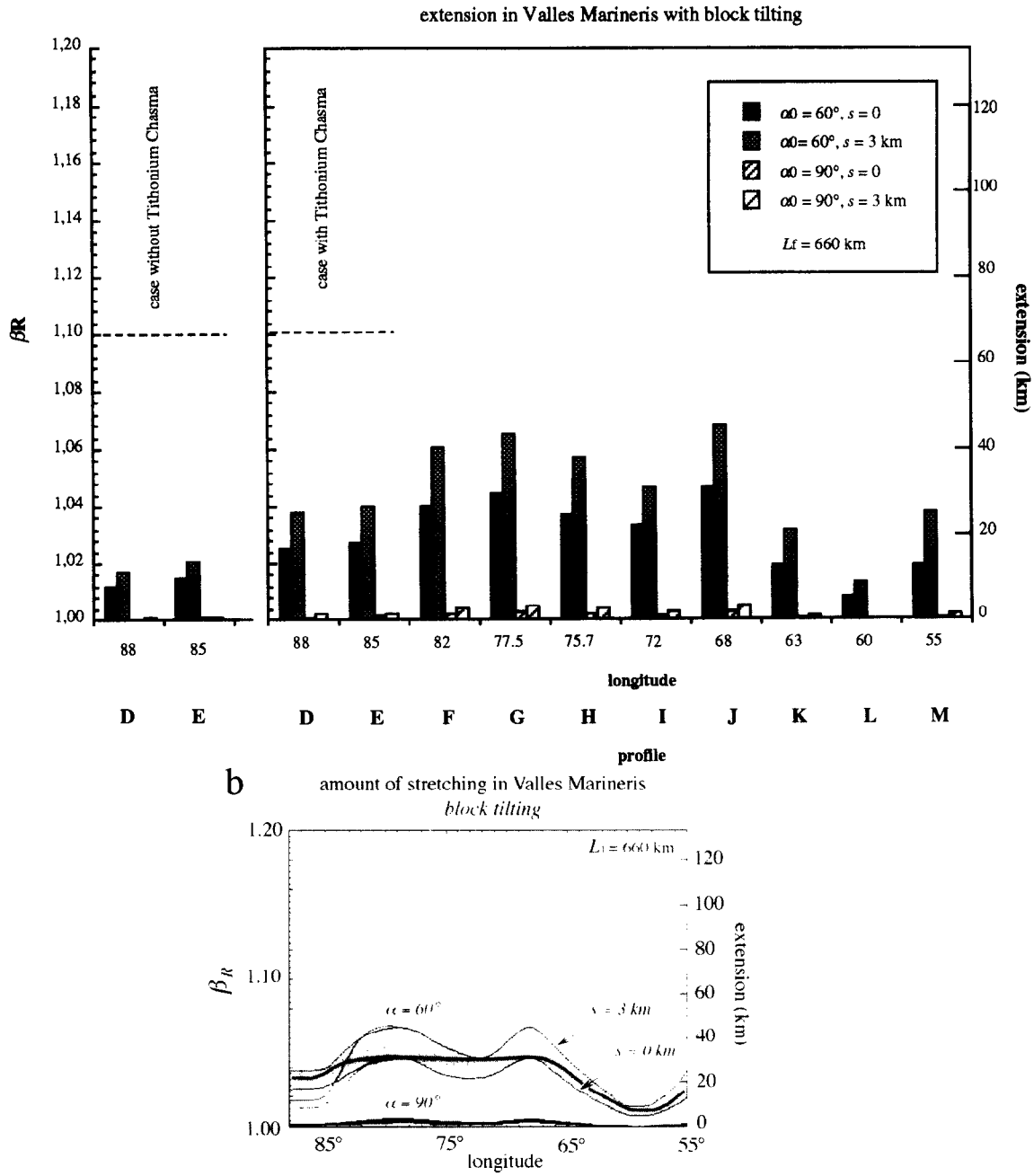

Fig. 14. (a) Extension of Valles Marineris assuming block tilting if all the faults have the same α_0 dip, with $\alpha_0 = 60°$ and 90°, and with $s = 0$ and 3 km. (b) Interpolation of the results presented in (a). Tectonic extension (dashed intervals) and no tectonic extension (light intervals eastward) in Tithonium Chasma are considered. The thick line in the dashed domain indicates a possible path for β (border faults expected to be 60° for convenient drawing but the interpretation is the same with different dip angles) indicating that despite the low stretching on profiles H and I, variations in sediment thickness allow to keep β constant and successfully correlate with the patterns of β variations in terrestrial continental rifts. This requires 3 km more sediments than in Ius and Coprates chasmata

5. Discussion

5.1. *Comparison to results from other works*

Other measurements of extension around Tharsis from Viking imagery, mainly for Hesperian structures, i.e. more or less contemporaneous to Valles Marineris, have been carried out by Plescia (1991) (Tharsis northern area), Chadwick and Lucchitta (1993) (Valles Marineris), Golombek *et al.* (1994, 1995a) (Sirenum Fossae, Tempe Terra), Golombek *et al.* (1995b) (Thaumasia Fossae), Tanaka and Golombek (1994) (Tempe Terra), and Schultz (1995) (Valles Marineris).

5.1.1. *Valles Marineris.* Schultz (1995) used a method similar to ours for calculating the variations of Valles Marineris stretching without block tilting. Both works were carried out independently. The range of border fault dips taken by Schultz (1995) is 50–70°. For 60°, he found extension values very similar to those we obtained when block tilting and sediments on the floors are neglected

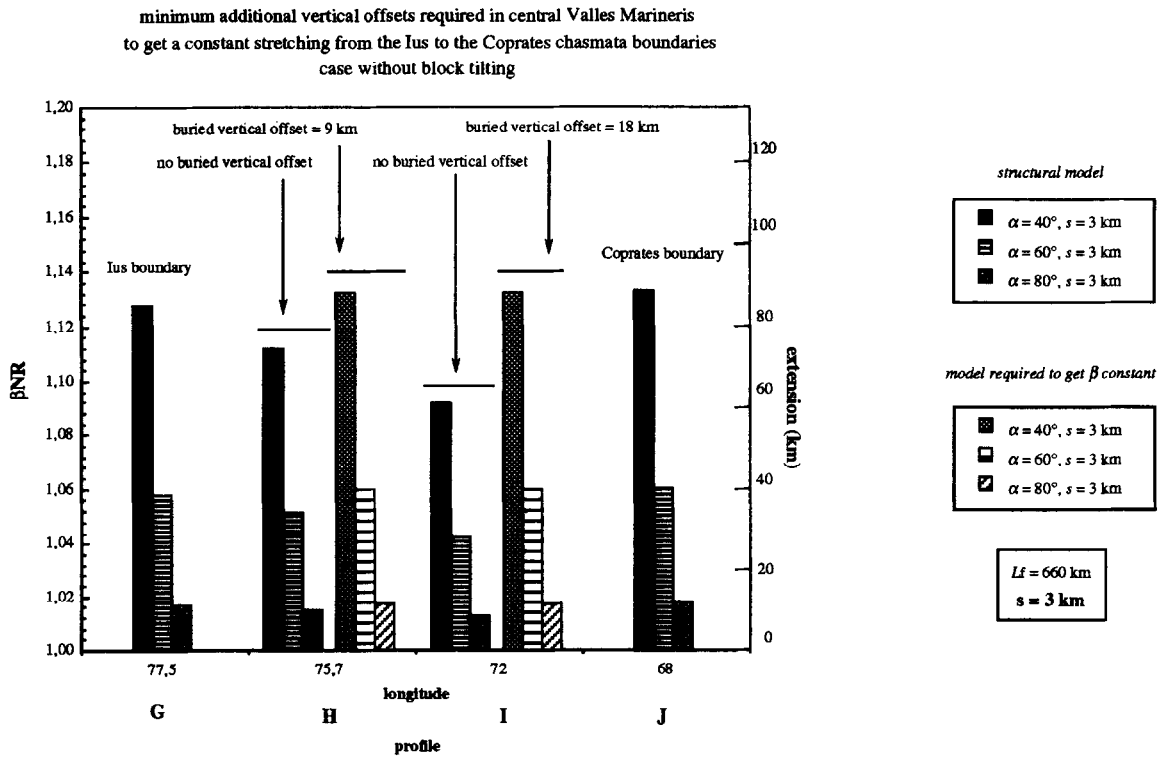

Fig. 15. Minimal additional vertical offsets required in central Valles Marineris in the non-rotational case to get constant stretching from the Ius to the Coprates chasmata boundaries

(Fig. 13a). Of particular interest is that his results show the same pattern of stretching variation along the grabens, including the increase of extension in Coprates Chasma toward the east. This pattern is observed even without taking stretching in Gangis Chasma into account. A difference however is that we standardized extension to a constant length profile (660 km), whereas he calculated strain at profiles of different length, including the deformed areas only. Therefore his strain values are more convenient for comparison with strain in other areas calculated the same way. This is particularly helpful because some boundaries between the stretched Tharsis

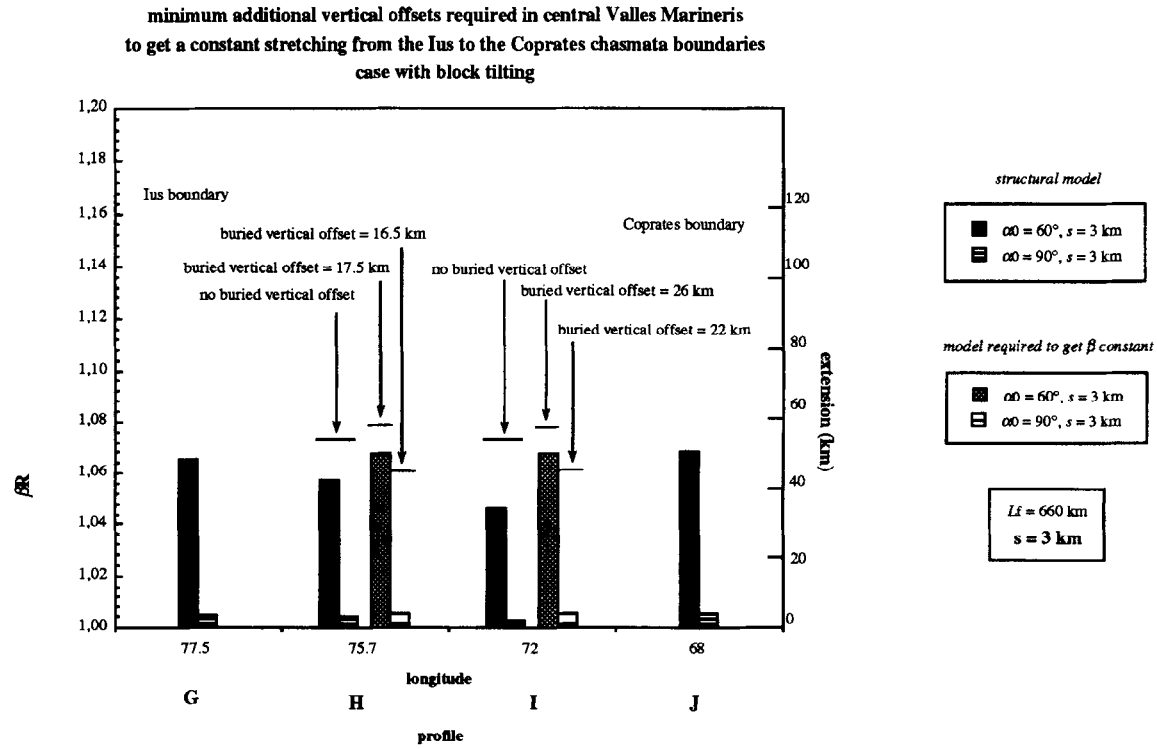

Fig. 16. Minimal additional vertical offsets required in central Valles Marineris in the rotational case to get constant stretching from the Ius to the Coprates chasmata boundaries

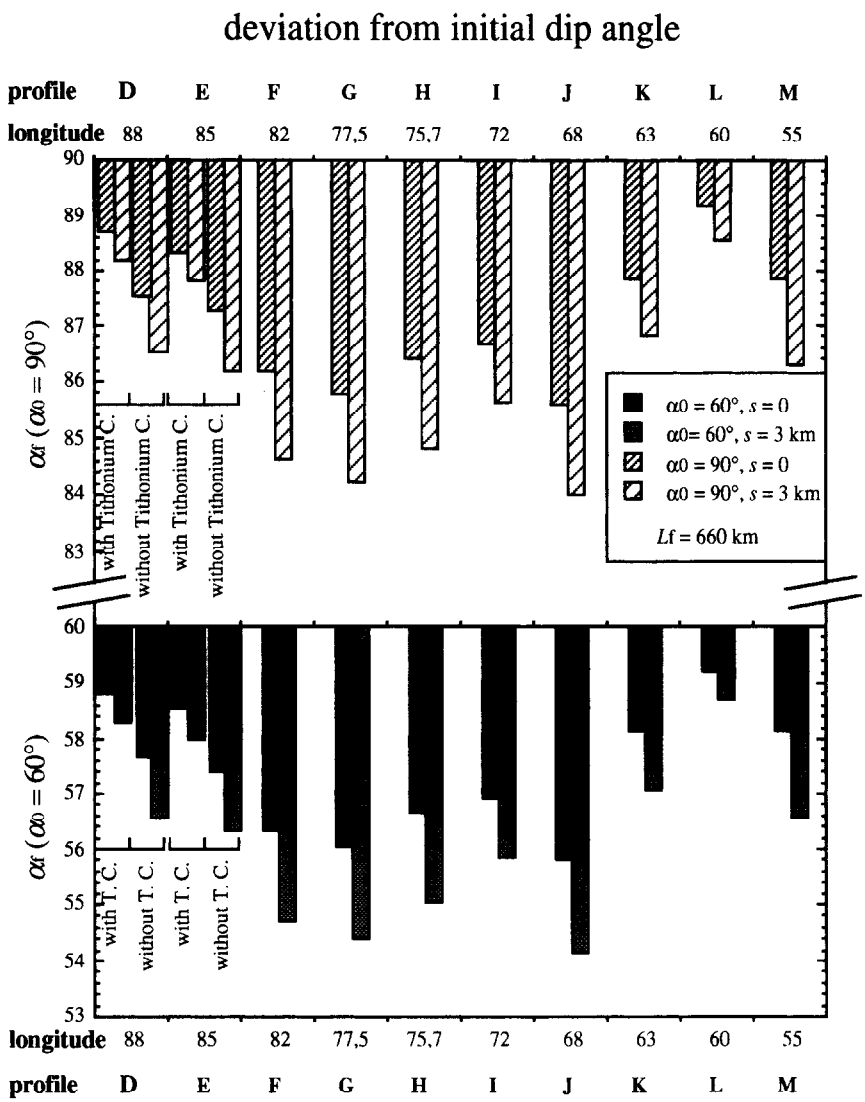

Fig. 17. Final dip angles α_f in the case of block tilting, assuming $\alpha_0 = 60°$ or 90

sub-provinces (see, e.g. Tanaka and Dohm, 1989) are partly arbitrary. They lie upon the assumption that the distribution of extensional radial patterns reflects the distribution of stress in the crust. The influence of crustal heterogeneities, such as provided by previous fracturing of various origin, by buried impact basins in the Tharsis hemisphere (Craddock *et al.*, 1990; Schultz and Frey, 1990; Frey and Roark, 1995); possible magmatic underplating or intra-crustal accretion; possible differences in crust density dating back to early crustal differentiation, etc. are neglected. Therefore, the notion of subprovinces is a convenient way to distinguish between Tharsis morphostructural units, but that all of them have a geodynamic significance cannot be assumed without caution. As a result, comparing strain between different subprovinces taking non-deformed areas into account is difficult.

Standardizing the results to the same profile length is nevertheless helpful when the possibility that the region submitted to the extensional forces is supposed to be larger than the region actually deformed is considered. In the Valles Marineris case, stretching could result from release of stress exerted in an array which may be much wider than the chasmata array. When the deformed arrays are considered only, the strain measured is well adapted to local Valles Marineris uplift, like would be produced by dynamic rifting. Taking the non-deformed arrays into account maybe more adapted to horizontal traction of the crust (passive rifting). Of course, in this respect, the 660 km length of our profiles is arbitrary, it could be considered as the minimum length of the array submitted to horizontal traction in the central Valles Marineris zone.

Chadwick and Lucchitta (1993) measured 35 km of extension across the widest part of Valles Marineris in the case the border faults are 60° dipping. This value is well within the range of our estimates around Melas Chasma, and corresponds to what we would expect if the mean bedrock depth below the floor sediments is close to 2 km. They found that extension would fall to 16 km in the case of 75° dipping faults, a result which is consistent with our estimates as well (Fig. 13a). If block rotation occurred, 75° dipping faults would correspond to roughly initially 80° dipping faults (Fig. 17). Although other mechanisms may explain such possible very steep dips, the formation of these faults from intruded joints, like in the Icelandic rift, where tectonic stretching results from some combination of horizontal traction of plate and stress related

to magma emplacement in the crust (Rubin, 1990; Forslund and Gudmundsson, 1991), is an attractive hypothesis.

5.1.2. *Other Tharsis subprovinces.* As noted above, recent works have given values of extension in other areas of Tharsis (Plescia, 1991; Golombek *et al.*, 1994, 1995a, b; Tanaka and Golombek, 1994). In a synthesis, Golombek *et al.* (1995b) estimate that the total extension around Tharsis should be 60 ± 46 km. The results presented here, and those presented by Schultz (1995), which unequivocally show that the amount of stretching recorded in the Valles Marineris chasmata varies along-strike, confirm the remark by Schultz that the mechanism of Valles Marineris stretching should be different from the mechanism of narrow radial graben formation, which appears not to have produced along-strike variations of stretching. According to Golombek *et al.* (1995b), some 44 ± 33 km of extension around Tharsis was not produced in Valles Marineris. Comparison with the results presented here suggests that the stretching mechanism for Valles Marineris formation could have been as efficient as that for radial graben formation. The uncertainty is however enormous, and the error bars, mainly due to the uncertainty on fault dips and to neglecting small-scale fracturing, cannot rule out the possibility that Valles Marineris absorbed four times more or 12 times less stretching than the other areas! This comparison between Valles Marineris and the other Tharsis subprovinces is however valid at the surface only. At more than a few hundred metres depth, the amount of stretching remains unknown, it depends in great part on whether tension cracks, dykes, or no joints, underlie the narrow radial grabens.

5.2. *Mechanisms of Valles Marineris formation*

Valles Marineris formation was the result of two possible basic mechanisms: uplift or horizontal traction. Following the terminology used for the Earth, uplift would lead to dynamic rifting, horizontal traction would lead to passive rifting (the most common case on Earth). In addition, Valles Marineris opening might also have been completed by extensional stress due to Tharsis loading.

5.2.1. *Dynamic rifting.* Dynamic rifting is consistent with most of the stretching variations observed (increasing stretching from the ends to the centre of the stretched system, provided the peak correction discussed above), but not with the increase of extension in Coprates Chasma eastward. It is also qualitatively consistent with the location of Valles Marineris on a secondary topographic bulge partially overlapping the main Tharsis bulge, which culminates at Syria Planum. The latter reaches 11 km in elevation, the former reaches 9 km (USGS, 1991, 1992). The Valles Marineris bulge is centred in the Echus/Hebes/Ophir/Candor area (Fig. 7), although some lower summits appear to exist as well. The correlation between the location of the top of the Valles Marineris bulge prior to extension and the trough depth cannot be established since it would require to accurately know sediment thicknesses in the chasmata. Nevertheless, as the location of the top of this bulge and the location of the deepest chasmata often correspond, Valles Marineris stretching and the formation of the bulge should be linked.

Nevertheless, as pointed out by Schultz and Senske (1995), the correspondence between the current uplift and the location of chasmata is quite unperfect. Furthermore, Chadwick and Lucchitta (1993) calculated that 4 km of elastic topographic bulging could not produce more than 1 km of circumferential extension, a value much smaller than all those calculated to date in Valles Marineris. Of course, the current bulge may not correspond to the bulge that existed at the onset of Valles Marineris stretching. Topographic uplift should have been stronger, due to thermal heating induced by upwelling below the rift, and it can be suggested that this could have been sufficient to produce the grabens by dynamic rifting (Chadwick and Lucchitta, 1993; Mège, 1994). An argument against this interpretation is however provided by comparison with the Earth, where rifting above a plume cannot result from the early doming effect of the plume. Plumes are highly efficient in crust weakening, but appear to be inefficient in producing rifts alone (Hill *et al.*, 1992).

5.2.2. *Passive rifting. Tectonic aspects.* Passive rifting can still not predict stretching of Gangis Chasma and the easternmost part of Coprates Chasma. A critical argument against passive rifting is that it requires horizontal traction, and subsequent shortening parallel to Valles Marineris in the surrounding plateaus if the source of extensional stress exerts in the Valles Marineris area only. Compressional structures around Valles Marineris are perpendicular to the direction of shortening expected if they were induced by Valles Marineris stretching (e.g. Watters and Maxwell, 1986). A recent study has provided new insights on the conditions of Valles Marineris development (Mège and Masson, 1995b, 1996b). Based on morphologic and structural arguments, that work demonstrates that many of the narrow radial grabens should have formed above giant swarms of dykes propagating throughout the Tharsis hemisphere from the Tharsis central areas from late Noachian up to Amazonian. The arguments given are mainly based on observations of interactions between dykes and ground water/ground ice throughout the Tharsis province, evidence of joint propagation associated with lava flows, analogy between secondary faults within the grabens and those obtained in analogical modelling of dyke emplacement with multiple pulses by Mastin and Pollard (1988), and frequent analogy between secondary tectonic patterns in the grabens and tectonic patterns induced by subsurface magma flow on Earth.

Dyke mapping revealed the existence of at least three giant dyke swarms in the Tharsis hemisphere. They were used to infer broad scale horizontal principal stress trajectories (e.g. Halls, 1987), whose geometric analysis indicates that a regional extensional stress system, independent of Tharsis, existed at least in the Tharsis hemisphere during the whole Hesperian, and at least part of Amazonian, and played a major role in the formation of the radial grabens. Valles Marineris, which formed contemporaneously to many of them, should have also been influenced by this stress field. Its orientation is indeed perpendicular to the direction of the regional least principal stress trajectory (N020E). Therefore a source for

horizontal traction of the Valles Marineris crust appeared to have existed, and is not contradictory with the lack of compressional structures parallel to the chasmata. The magnitude of the regional deviatoric stress was strong enough to produce the narrow grabens. For instance, it was enough to produce 22 ± 16 km of surface stretching in Tempe Terra (Golombek *et al.*, 1995a), a value which is of the same order as extension values obtained in Valles Marineris (Schultz (1995) and this study). Consequently, this stress source should have contributed to form the chasmata as well.

A reason for the difference in tectonic style between Valles Marineris and the grabens elsewhere around Tharsis must however be found (Schultz, 1995). Giant radiating dyke swarms appear to have frequently formed in response to hot spots on Earth (Fahrig, 1987; LeCheminant and Heaman, 1989; Ernst *et al.*, 1995), which have a weakening effect on the crust that is strong enough to trap terrestrial rifts (White and McKenzie, 1989; Hill *et al.*, 1992). Rift location is governed by the geometry of the weakened crust. Rift geometry is a compromise between regional stress trajectory and previous fracturing. At large scale, this generally means that the rift follows the skeleton given by those dykes that are perpendicular to the regional least principal stress trajectory (Fahrig, 1987). This evolution appears to have been thoroughly followed by Valles Marineris, which formed just after a graben and dyke swarm centred on Syria Planum (from data in Tanaka (1986), Tanaka and Davis (1988), and Mège (1994) corresponding in location to the Syria Planum fracturing centre of Plescia and Saunders (1982)). Its existence, location, and geometry, are predicted by the existence of both (1) the plume centred on Syria Planum, and the associated dyke swarm, and (2) the regional extensional stress source. More details can be found in Mège and Masson (1995a, b, 1996b), and a detailed discussion of the model is given by Mège and Masson (1996b). Correlation between the model and other tectonic features is out of the scope of this paper. However, in order to make the passive rifting interpretation stronger, it is worthwhile to note that it is also consistent with (1) the upper Noachian/lower Hesperian south Tharsis ridge belt (Schultz and Tanaka, 1994), expected to be due to stress at the boundary between the uplifted and non-uplifted area around plume (Price and Cosgrove, 1990); and (2) the location and orientation of wrinkle ridges, due to local subsidence of the weakened and thinned brittle crust under the load of the lava floods (Hill *et al.*, 1992) within the stress context that presided to narrow graben and Valles Marineris formation. In this respect, the critical points mentioned by Watters (1993) are better fitted than previous hypotheses for wrinkle ridge formation in the Tharsis hemisphere yet published, and the model is also in good agreement with stratigraphic studies (Tanaka, 1986; Tanaka and Dohm, 1994).

Magmatic aspects. The model is particularly consistent with the uplifted plateaus surrounding Valles Marineris. The uplift of the central and eastern part has been found to be consistent with rift shouldering due to unloading (Schultz and Senske, 1995). It is however insufficient to explain the topography closer to Syria Planum. This should be solved in considering the simple model of partial melting in stretched regions (McKenzie and Bickle, 1988; White and McKenzie, 1989; McKenzie and O'Nions, 1991). According to the results obtained by McKenzie and O'Nions, with a classical terrestrial mantle temperature (1300°C), and taking the acceleration of gravity to be $3.71\ m\ s^{-2}$, thinning a 140 km thick Valles Marineris mechanical lithosphere is enough to generate partial melting by adiabatic mantle decompression. Twelve per cent partial melting is generated if lithosphere thickness is decreased to 50 km, corresponding to a total thickness of molten materials equal to 7 km. If effects of a typical plume, inducing a 200°C thermal anomaly, are added, partial melting starts for a mechanical lithosphere thickness of 300 km, and lithosphere thinning to 50 km results in more than 25% partial melting (a tholeiitic basalt composition), and a total thickness of molten materials equal to 45 km. For comparison, the current Martian elastic lithosphere thickness is often estimated to 150 km, suggesting that the mechanical lithosphere thickness could be of the order of, e.g. 200 km. It should have been much less when Valles Marineris formed.

Overall, magmatic underplating and intrusion to the Valles Marineris crust (depending on the magma density), which has been scarcely discussed in the literature, should probably be viewed as a necessary and major aspect of Valles Marineris evolution. Magma accretion should have contributed to plateau uplift, similar to several uplifted continental regions with abnormally thick crust on Earth (McKenzie, 1984), including around continental rifts (e.g. McDonald and Upton, 1993), especially in the regions close to the Syria Planum, where unloading cannot explain the high topography. Nevertheless, the model in Mège and Masson (1995b, 1996b) predicts that it should have also contributed, to a somewhat smaller extent, to uplift of the central and eastern parts of Valles Marineris as well.

Location of tectonic and magmatic events. The imperfect correspondence between the location of chasmata and that of the uplifted plateaus has been argued against the dynamic rifting interpretation. This argument does not stand for passive rifting, because, basically, rift structure in the upper crust and partial melting in the asthenosphere are actually very different processes (upper crustal rifting and mantle decompression, respectively), although linked by the same root cause (extensional stress applied to the lithosphere). Logatchev (1993) pointed out that the location of the Baikal rift geologic structures and that of most intense magmatism are different, although both are a consequence of the same geodynamics.

Gravity. Magma accretion to the Valles Marineris crust is consistent with gravity data computed by Smith *et al.* (1993), which denote (despite high uncertainties discussed by these authors) a negative anomaly below the central troughs, suggesting that they are not in isostatic state, in contrast to the surrounding volcanic plateaus and cratered highlands (Frey *et al.*, 1995).

These data are in agreement with the passive rifting hypothesis. Magma extraction from the mantle is a dominantly vertical process. It results in a low-density residuum underlying the intruded lithosphere, which contributes to maintain a high topography in rifted regions during stretching (White and McKenzie, 1989). Once the magma in the lithosphere has frozen, assuming that there is no

lateral loss of the residuum in the surrounding mantle, the gravity anomaly is negative. This is because although the high magma density may be counterbalanced by the low residuum density, crust unloading due to stretching produces a negative anomaly. At longer term, a natural trend to subsidence exists. However, if creep of the residuum to the surrounding mantle is difficult, subsidence can be impeded or prevented. In planets smaller than the Earth, viscosity increase in the upper mantle with planet cooling should be a process more rapid than on Earth. Consequently, rift subsidence should be more easily impeded or prevented than it would be on Earth, leading to a long-lasting or permanent flexural uplift, or to partial compensation, which could explain why more than 2 Ga after its main formation stage, Valles Marineris is currently not in isostatic state.

Some of the magma produced below Valles Marineris could provide a basis to the hypotheses favouring a volcanic origin and alkalic composition for the layered deposits (Nedell, 1987). These volcanic rocks would have likely not played a substantial role in Valles Marineris uplift attenuation, owing to their low density.

5.2.3. *Tharsis loading.* In the models of loading available to date, the load is considered axisymmetric and be exerted on an elastic plate. The load centre corresponds to the Tharsis centre, therefore, the mechanism for Valles Marineris stretching is very different from dynamic or passive rifting.

Stress models. Many works on the Tharsis state and evolution of stress have been carried out for 20 years (reviews in Banerdt *et al.* (1992) and Mège and Masson (1996a)). Banerdt *et al.* (1982) particularly focused part of their study to the Valles Marineris case. These works show that the topography and gravity data are consistent with three styles of support. Tharsis could be dynamically supported by flexural uplift (due to mantle upwelling for instance), or by the volcanic, and, above all, the plutonic load (Phillips *et al.*, 1973; Willemann and Turcotte, 1982; Finnerty *et al.*, 1988; Phillips *et al.*, 1990). Both isostasy (Pratt + Airy) and flexural loading were investigated.

The comparison between stress related to the Tharsis dome and the development of Valles Marineris led to the conclusion that Tharsis dynamic uplift produces stresses which are inconsistent with trough orientation. Isostatic stresses in elastic models are consistent with the formation of the western Valles Marineris troughs, but inconsistent with the formation of the eastern troughs. Conversely, flexural Tharsis loading could explain the development of the eastern troughs only. Many authors thus concluded that the Tharsis region would be primarily supported by isostatic forces, and increasing of the brittle lithosphere thickness would have led to a flexural support (e.g. Banerdt *et al.*, 1982; Solomon and Head, 1982; Sleep and Phillips, 1985).

As isostasy and flexural loading are two different states of the same support mode (loading), the transition from one to the other is gradual, and may be considered as a single process which may have been completed in a few ten or hundred million years. Stratigraphic relationships (Scott and Tanaka, 1986; Witbeck *et al.*, 1991) and style of tectonic recording on walls (e.g. Peulvast *et al.*, 1996) show that graben formation in Valles Marineris mainly

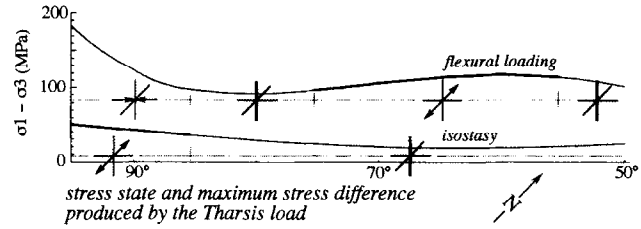

Fig. 18. Variation of isostatic and flexural loading stress states (extension, strike slip, compression—north is approximately as indicated) and magnitudes along Valles Marineris at 10°S, extrapolated from Banerdt *et al.* (1992). Thick lines underline the extensional domains predicted by Banerdt *et al.* (1992)

took place during upper Hesperian. Upper Hesperian may have lasted 150–1300 Ma (Neukum and Wise, 1976; Hartmann *et al.*, 1981). Therefore, replacement of isostatic to flexural support may have wholly taken place between the lower and upper bounds of upper Hesperian. Opening of western chasmata would have taken place earlier than opening of the eastern chasmata, but no morphologic nor structural clue for this two-stage evolution could be currently observed.

For the opposite case, the detached crustal cap model of Banerdt and Golombek (1990) and Tanaka *et al.* (1991) allows all the chasmata to form simultaneously. The upper crust of the internal regions of Tharsis would be decoupled from the brittle upper mantle by a lower ductile crust, leading to a mode of support responsible for stresses roughly corresponding to the ones that would be produced by isostasy (Airy) at a crustal scale. The ductile part of the crust would lack in the external part of the dome owing to a thinner (less intruded) crust and a weaker thermal gradient. The crust and the lithospheric mantle would be coupled, and the isostatic-like state could not be reached. The western and eastern part of Valles Marineris could thus have formed at the same time, but under different governing processes. This scenario is temptative for Valles Marineris, it is in addition in good agreement with the works by Allemand *et al.* (1989) and Buck (1991) disucssed in Section 2.5. Nevertheless, under its present form, it still encounters structural inconsistencies in other Tharsis subprovinces (Watters, 1993; Mège and Masson, 1996a).

Stress states and magnitudes. The stress states and magnitudes predicted by elastic models across Valles Marineris are displayed on Fig. 18 (extrapolated from data in Banerdt *et al.* (1992)). Comparison with Figs 13a and 14a, and with Fig. 3 in Schultz (1995) suggests a rather poor correlation between the along-strike variations of stretching obtained in this study and in Schultz (1995), and the theoretical variations.

From a stress state point of view, considering combination of isostatic and flexural stress states in a way to reproduce the detached crustal cap model cannot provide satisfying fit, because a strike-slip domain remains at the Valles Marineris centre. However McGovern and Solomon (1993) and Schultz and Zuber (1992, 1994) showed that stretching can occur in regions where strike-slip is predicted in elastic models, because of the influence of early stages of fracturing on later stages of fracturing during load growth. Taking this remark into account, the

stress state predicted by the detached crustal cap model may explain the Valles Marineris formation.

The variations of stretching obtained in this study are more difficult to correlate with the variations of stress magnitudes on Fig. 18, basically because elastic modelling of stress considers the present Tharsis characteristics. The computed magnitudes would make sense if Tharsis building was an instantaneous loading process, and, consequently, the lithosphere would have to be an infinite strength. Indeed tension failure occurs for a few MPa in traction (e.g. ~5 MPa for the volcanic substratum of Iceland (Bäckström and Gudmundsson, 1989); see also Schultz (1993)), whereas the maximum stress difference at the surface computed by Banerdt *et al.* (1992) predicts 20–60 MPa in the Tharsis area and surroundings in the isostatic case, and 50–250 MPa in the flexural case. The computations by Banerdt *et al.* (1982) and Sleep and Phillips (1985) gave about the same results. Schultz and Zuber (1994) emphasized that the evolution of stress state in a fractured medium is not linear, and thus the computed stress cannot be extrapolated to find the initial failure characteristics. Since Tharsis gradually built up over Hesperian and Amazonian, the variations of stretching that would have resulted from loading stress might thus be different to those predicted in Fig. 18. Overall, it is thus not possible to say whether loading stress states and magnitudes provided by current loading models are in agreement with the results given in this study or not, because the kind of results of those studies mainly deal with stress, and ours mainly deal with strain.

Stress trajectories. The discrepancy between stress and strain in Valles Marineris also applies to the comparison between theoretical stress trajectories and observations of stretching direction. This might explain that the westernmost parts of Ius and Tithonium chasmata are not consistent with the theoretical stress trajectories. The latter predict the principal most compressive stress to be NE–SW, in contradiction with the N–S border faults.

Except in this part of Valles Marineris, loading models are consistent with the general N105°E Valles Marineris trend, from Ius Chasma westward up to Gangis Chasma, and even with the easternmost part of Coprates Chasma where this trend becomes N090. This feature is not predicted by simple models of rifting discussed above—although it is not a major problem to the rift interpretation, since previous N090 discontinuities in the crust, such as tension fractures or dykes, could have existed and influenced the geometry of rifting.

5.3. *Synthesis*

Valles Marineris formed essentially during Hesperian. No recent major magmatic activity has been observed in the close surroundings (Syria Planum area) after Valles Marineris formation (Tanaka (1986); however minor magmatic activity undoubtly took place more recently in Valles Marineris (Lucchitta, 1990)). Therefore, this part of the Tharsis province should produce loading stress for a long time, maybe since lower Amazonian.

In contrast, formation of the Tharsis Montes, lava flooding throughout Amazonian around these volcanoes, and clues of simultaneous or later radiating dyke propagation (Tanaka and Golombek, 1989; Tanaka *et al.*, 1991; Mège, 1994; Davis *et al.*, 1995; Mège and Masson, 1995b, d), require some magmatic fluid chambers very recently in the Mars history (Tanaka, 1986). As a consequence, the magmatic load of Tharsis should have been negligible during the formation of Valles Marineris.

It is consequently possible to propose a mechanism for Valles Marineris formation involving both dynamic and loading processes. We suggest that most of Valles Marineris formed following the passive rifting mechanism discussed in Section 5.2.2. On Earth lithospheric loads are responsible for stress that produces tectonic deformations in several ways (Mercier *et al.*, 1981; Fleitout, 1991; Assumpçao, 1992; Zoback, 1992). It would thus not be surprising for the magma loads of the Tharsis region to have contributed to Valles Marineris stretching, but mainly after the end of the rifting process (Grana and Richardson, 1996; Zoback and Richardson, 1996). The deformations associated with these loads could include some recent tectonic movements in Valles Marineris, especially some of those that were not eroded in spurs and gullies (maps in Peulvast *et al.* (1996)).

Acknowledgements. Thanks to Jean-Pierre Peulvast, Richard Schultz, Denis Sorel, Pierre Vergely, Yue Qiao Zhang, Pascal Allemand and Tony Cook for helpful discussions. Thanks to Thierry Souriot and Jean-Pierre Brun for helpful comments during early stages of elaboration of the manuscript, which also benefited from reviews by Jouko Raitala and an anonymous referee. Thanks to Jan-Peter Muller for permission to use the UCL Ius and Tithonium chasmata DEM. This paper represents a research effort supported by Programme National de Planétologie from Institut National des Sciences de l'Univers (CNRS, France). The data used in this study were made available by the Regional Planetary Image Facility at Université Paris-Sud (Orsay, France) under the auspices of NASA Planetary Geology and Geophysics Program.

References

Allemand, P. and Brun, J. P., Width of continental rifts and rheological layering of the lithosphere. *Tectonophysics* **188,** 63–69, 1991.

Allemand, P., Brun, J. P., Davy, P. and Van Den Driessche, J., Symétrie et asymétrie des rifts et mécanismes d'amincissement de la lithosphère. *Bull. Soc. Géol. Fr.* **8**(3), 445–451, 1989.

Anderson, E. M., *The Dynamics of Faulting and Dyke Formation with Applications to Britain*, 2nd edn, 206 pp. Oliver & Boyd, Edinburgh, 1951.

Anderson, F. S. and Grimm, R. E., Lithospheric controls on the formation of Valles Marineris. *Lunar Planet. Sci. Conf.*, Vol. XXV, pp. 29–30. Lunar and Planetary Institute, Houston, 1994.

Anderson, F. S. and Grimm, R. E., Crustal thickness variations at Valles Marineris, Mars. *Lunar Planet. Sci. Conf.*, Vol. XXVI, pp. 39–40. Lunar and Planetary Institute, Houston, 1995.

Angelier, J. and Coletta, B., Tension fractures and extensional tectonics. *Nature* **301**(5895), 49–51, 1983.

Angelier, J., Faugère, E., Michel-Noël, G. and Anderson, R. E., Bassins en extension et tectonique synsédimentaire, exemples

dans les "Basin and Range" (U.S.A.), Total CFP. *Notes et mémoires* **21**, 51–72, 1986.

Assumpçao, M., The regional intraplate stress field in South America. *J. Geophys. Res.* **97**(B8), 11889–11903, 1992.

Bäckström, K. and Gudmundsson, A., The grabens of Sveinar and Sveinagja, NE Iceland, Nordic Volcanological Institute 8901, University of Iceland, Reykjavik, 38 pp. + detailed structural map, 1989.

Banerdt, W. B. and Golombek, M. P., The evolution of Tharsis: implications of gravity, topography, and tectonics, in MEVTV: scientific results of the NASA-sponsored study project on Mars: evolution of volcanism, tectonics, and volatiles, LPI Technical Rept No. 90-06, Lunar and Planetary Institute, Houston, 1990.

Banerdt, W. B., Phillips, R. J., Sleep, N. H. and Saunders, R. S., Thick shell tectonics on one-plate planets: application to Mars, *Proc. 3rd International Colloquium on Mars. J. Geophys. Res.* **87**(B12), 9723–9733, 1982.

Banerdt, W. B., Golombek, M. P. and Tanaka, K. L., Stress and tectonics on Mars, in *Mars* (edited by Kiefer *et al.*), pp. 249–297. University of Arizona Press, Tucson, 1992.

Barr, D., Lithospheric stretching, detached normal faulting and footwall uplift, in *Continental Extensional Tectonics* (edited by M. P. Coward, J. F. Dewey and P. L. Hancock), Geol. Soc. Sp. Publ. 28, pp. 75–94, 1987.

Blasius, K. R., Cutts, J. A., Guest, J. E. and Masursky, H., Geology of the Valles Marineris: first analysis of imaging from the Viking 1 Orbiter primary mission. *J. Geophys. Res.* **82**(28), 4067–4091, 1977.

Bois, C., Initiation and evolution of the Oligo–Miocene rift basins of southwestern Europe: contribution of deep seismic reflection profiling. *Tectonophysics* **226**, 227–252, 1993.

Brun, J. P. and Choukroune, P., Normal faulting, block tilting, and décollement in a stretched crust. *Tectonics* **2**(4), 345–356, 1983.

Brun, J. P., Gutscher, M.-A. and the DEKORP–ECORS teams, Deep crustal structure of the Rhine Graben from DEKORP–ECORS seismic reflection data: a summary. *Tectonophysics* **208**, 139–147, 1992.

Buck, W. R., Flexural rotation of normal faults. *Tectonics* **7**(5), 959–973, 1988.

Buck, W. R., Modes of continental lithospheric extension. *J. Geophys. Res.* **96**(B12), 20161–20178, 1991.

Buck, W. R., Effect of lithospheric thickness on the formation of high- and low-angle normal faults. *Geology* **21**, 933–936, 1993.

Byerlee, J. D., Friction of rocks. *Pure Appl. Geophys.* **116**(415), 615–626, 1978.

Carr, M. H., Tectonism and volcanism of the Tharsis region of Mars. *J. Geophys. Res.* **79**(26), 3943–3949, 1974.

Carr, M. H., *The Surface of Mars*, Planetary Exploration Series, 232 pp. Yale Univ. Press, 1981.

Chadwick, D. J. and Lucchitta, B. K., Fault dips in the Valles Marineris: a photogrammetric study. *Lunar Planet. Sci. Conf.*, Vol. XXIII, pp. 221–212. Lunar and Planetary Institute, Houston, 1992.

Chadwick, D. J. and Lucchitta, B. K., Fault geometries and extension in the Valles Marineris, Mars. *Lunar Planet. Sci. Conf.*, Vol. XXIV, pp. 263–264. Lunar and Planetary Institute, Houston, 1993.

Chicarro, A. F., Schultz, P. H. and Masson, P., Global and regional ridge patterns on Mars. *Icarus* **63**, 153–174, 1985.

Chorowicz, J., Transfer and transform fault zones in continental rifts: examples in the Afro-Arabian Rift System. Implications of crust breaking. *J. Afr. Earth Sci.* **8**(2–4), 203–214, 1989.

Chorowicz, J., Guezlane, M., Rudant, J. P. and Vidal, G., Analyse de la zone de failles d'Assoua au Kenya à partir des images spatiales Landsat-MSS et MOMS-01. Influence de l'héritage précambrien sur la structure du Gregory Rift. *C. R. Acad. Sci. Paris* **307**(II), 83–84, 1988.

Chorowicz, J., Desffontaines, B. and Villemin, T., Interprétation des structures transverses NE–SW du fossé rhénan en termes de failles de transfert. Apport de données multisources. *C. R. Acad. Sci. Paris* **309**(II), 1067–1073, 1989.

Costard, F., Distribution et caractéristiques du pergélisol sur Mars: son influence sur certains traits de la géomorphologie, Thèse de doctorat, Laboratoire de géographie physique, URA D0141, 327 pp., Université Paris IV, Meudon, France, 1990a.

Costard, F., Vallées de débâcle et processus cryokarstiques sur Mars et en Sibérie (in French with English abstract and captions). *Géogr. Phys. Quaternaire* **44**(1), 97–104, 1990b.

Costard, F. M. and Kargel, J. S., Outwash plains and thermokarst on Mars. *Icarus* **114**, 93–112, 1995.

Craddock, R. A., Greeley, R. and Christensen, P. R., Evidence for an ancient impact basin in Daedalia Planum, Mars. *J. Geophys. Res.* **95**(B7), 10729–10741, 1990.

Daly, M. C., Chorowicz, J. and Fairhead, J. D., Rift basin evolution in Africa: the influence of reactivated steep basement shear zones, in *Inversion Tectonics* (edited by M. A. Cooper and G. D. Williams), Geol. Soc. Sp. Publ. 44, pp. 309–334, 1989.

Davis, P. A., Tanaka, K. L. and Golombek, M. P., Topography of closed depressions, scarps, and grabens in the north Tharsis region of Mars: implications for shallow crustal discontinuities and graben formation. *Icarus* **114**, 403–422, 1995.

Day, T., Cook, A. C. and Muller, J. P., Automated digital topographic mapping techniques for Mars, in *Int. Archives Photogrammetry Remote Sensing* (edited by L. W. Fritz and J. R. Lucas), Vol. 29, No. B4, pp. 801–808, 1992.

Dresen, G., Gwildis, U. and Kluegel, T., Numerical analogue modelling of normal fault geometry, in *The Geometry of Normal Faults* (edited by A. M. Roberts, G. Yielding and B. Freeman), Geol. Soc. Sp. Publ. 56, pp. 207–217, 1991.

Ernst, R. E., Buchan, K. L. and Palmer, H. C., Giant dyke swarms: characteristics, distribution and geotectonic applications, in *Physics and Chemistry of Dykes* (edited by G. Baer and A. Heimann), *Proc. 3rd Int. Dyke Conf.*, Jerusalem, September 4–8, 1995, Balkema, Rotterdam, pp. 3–21, 1995.

Fahrig, W. F., The tectonic settings of continental mafic dyke swarms: failed arm and early passive margin, in *Mafic Dyke Swarms* (edited by H. C. Halls and W. F. Fahrig), *Proc. Int. Conf.*, Erindale College, Univ. Toronto, June 4–7, 1985, Geol. Assoc. Canada Sp. Pap. 34, pp. 331–348, 1987.

Finnerty, A. A., Phillips, R. J. and Banerdt, W. B., Igneous processes and closed system evolution of the Tharsis region of Mars. *J. Geophys. Res.* **93**(B9), 10225–10235, 1988.

Fleitout, L., The sources of lithospheric tectonic stress, in *Tectonic Stress in the Lithosphere* (edited by R. B. Whitmarsh, M. H. P. Bott, J. D. Fairhead and N. J. Kusznir). *Phil. Trans. R. Soc. Lond.* **337**, 73–81, 1991.

Forslund, T. and Gudmundsson, A., Crustal spreading due to dikes and faults in southwest Iceland. *J. Struct. Geol.* **13**(40), 443–457, 1991.

Forslund, T. and Gudmundsson, A., Structure of Tertiary and Pleistocene normal faults in Iceland. *Tectonics* **11**(1), 57–68, 1992.

Frey, H. V., Martian canyons and African rifts: stuctural comparisons and implications. *Icarus* **37**, 142–155, 1979.

Frey, H. V. and Roark, J. H., A multi-ring impact basin in Thaumasia. *Lunar Planet. Sci. Conf.*, Vol. XXVI, pp. 425–426. Lunar and Planetary Institute, Houston, 1995.

Frey, H. V., Bills, B. G. and Nerem, R. S., The isostatic state of Martian topography—revisited. *Lunar Planet. Sci. Conf.*, Vol. XXVI, pp. 427–428. Lunar and Planetary Institute, Houston, 1995.

Gawthorpe, R. L. and Hurst, J. M., Transfer zones in extensional basins their structural style and influence on drainage development and stratigraphy. *J. Geol. Soc. Lond.* **150**, 1137–1152, 1993.

Golombek, M. P., Tanaka, K. L., Chadwick, D. J., Franklin, B. J. and Davis, P. A., Extension across Tempe Terra and Sirenum provinces on Mars from measurements of fault scarp widths. *Lunar Planet. Sci. Conf.*, Vol. XXV, pp. 443–444, 1994.

Golombek, M. P., Davis, P. A., Banerdt, B. and Franklin, B. J., Extension across tension cracks and tensile strength of shallow crustal materials on Mars. *Lunar Planet. Sci. Conf.*, Vol. XXVI, pp. 477–478, 1995a.

Golombek, M. P., Franklin, B. J., Tanaka, K. L., Dohm, J. M. and Banerdt, W. B., Extension across Thaumasia and around Tharsis on Mars. *Lunar Planet. Sci. Conf.*, Vol. XXVI, pp. 479–480, 1995b.

Grana, J. P. and Richardson, R. M., Tectonic stress in the New Madrid seismic zone. *J. Geophys. Res.* **101,** 5445–5458, 1996.

Greeley, R. and Iversen, J. D., *Wind as a Geological Process on Earth, Mars, Venus and Tritan*, 333 pp. Cambridge Univ. Press, Cambridge, 1985.

Gudmundsson, A., Formation and growth of normal faults at the divergent plate boundary in Iceland. *Terra Nova* **4,** 464–471, 1992.

Gudmundsson, A., The geometry and growth of dykes, in *Physics and Chemistry of Dykes* (edited by G. Baer and A. Heimann), *Proc. 3rd Int. Dyke Conf.*, Jerusalem, September 4–8, 1995, Balkema, Rotterdam, pp. 23–34, 1995.

Gudmundsson, A. and Bäckström, K., Structure and development of the Sveinagja graben, northeast Iceland. *Tectonophysics* **200,** 111–125, 1991.

Halls, H. C., Dyke swarms and continental rifting: some concluding remarks, in *Mafic Dyke Swarms* (edited by H. C. Halls and W. F. Fahrig), *Proc. Int. Conf.*, Erindale College, Univ. Toronto, June 4–7, 1985, Geol. Assoc. Canada Sp. Pap. 34, pp. 483–492, 1987.

Hartmann, W. K., Strom, R. G., Weidenschilling, S. J., Blasius, K. R., Woronov, A., Dence, M. R., Grieve, R. A. F., Diaz, J., Chapman, C. R., Shoemaker, E. M. and Jones, K. L., Chronology of planetary volcanism by comparative studies of planetary cratering, in *Basaltic Volcanism on the Terrestrial Planets* (edited by Members of the Basaltic Volcanism Study Project), pp. 1049–1127. Pergamon Press, Oxford, 1981.

Hetzel, R. and Strecker, M. R., Late Mozambique Belt structures in western Kenya and their influence on the evolution of the Cenozoic Kenya Rift. *J. Struct. Geol.* **16**(2), 189–201, 1994.

Hill, R. I., Campbell, I. H., Davies, G. F. and Griffiths, R. W., Mantle plumes and continental tectonics. *Science* **256,** 1186–1193, 1992.

Jackson, J. A., Active normal faulting and crustal extension, in *Continental Extensional Tectonics* (edited by M. P. Coward, J. F. Dewey and P. L. Hancock), Geol. Soc. Sp. Publ. 28, pp. 3–17, 1987.

Jackson, J. A. and McKenzie, D. P., The geometrical evolution of normal fault systems. *J. Struct. Geol.* **5**(5), 471–482, 1983.

Keen, C., Peddy, C., de Voogd, B. and Matthews, D., Conjugate margins of Canada and Europe: results from deep reflection profiling. *Geology* **17,** 173–176, 1989.

Kiefer, W. S. and Johnson, M. S., Physical properties controlling the style of extensional deformation in the Tharsis region of Mars. *Lunar Planet. Sci. Conf.*, Vol. XXVI, pp. 741–742. Lunar and Planetary Institute, Houston, 1995.

Klemperer, S. L., Crustal thinning and nature of extension in the northern North Sea from deep seismic reflection profiling. *Tectonics* **7**(4), 803–821, 1988.

Kokelaar, P., Magma–water interactions in subaqueous and emergent basaltic volcanism. *Bull. Volcanol.* **48,** 275–289, 1986.

Kusznir, N. J., Marsden, G. and Egan, S. S., A flexural-cantilever simple-shear/pure-shear model of continental lithosphere extension: applications to the Jeanne d'Arc Basin, Grand Banks and Viking graben, North Sea, in *The Geometry of Normal Faults* (edited by A. M. Roberts, G. Yielding and B. Freeman), Geol. Soc. Sp. Publ. 56, pp. 41–60, 1991.

LeCheminant, A. N. and Heaman, L. M., Mackenzie igneous events, Canada: middle Proterozoic hotspot magmatism associated with ocean opening. *Earth Planet. Sci. Lett.* **96,** 38–48, 1989.

Lin, J. and Parmentier, E. M., A finite amplitude necking model for the formation and evolution of rift zones in a brittle lithosphere. *J. Geophys. Res.* **95**(B4), 4909–4923, 1990.

Lockner, D. A., Byerlee, J. D., Kuksenko, V., Ponomarev, A. and Sidorin, A., Quasi-static fault growth and shear fracture energy in granite. *Nature* **350,** 39–42, 1991.

Logatchev, N. A., History and geodynamics of the Lake Baikal rift in the context of the Eastern Siberia Rift System: a review. *Bull. Centres Rech. Explor.-Prod. Elf Aquitaine* **17**(2), 353–370, 1993.

Lorenz, V., On the growth of maars and diatremes and its relevance to the formation of tuff rings. *Bull. Volcanol.* **48,** 265–274, 1986.

Lucchitta, B. K., Young volcanic deposits in the Valles Marineris, Mars? *Icarus* **86,** 476–509, 1990.

Lucchitta, B. K., McEwen, A. S., Clow, G. D., Geissler, P. E., Singer, R. B., Schultz, R. A. and Squyres, S. W., The canyon system on Mars, in *Mars* (edited by W. S. Kiefer *et al.*), pp. 453–492. Univ. Arizona Press, Tucson, 1992.

McDonald, R. and Upton, B. G. J., The Proterozoic Gardar rift zone, south Greenland: comparisons with the East African Rift System, in *Magmatic Processes and Plate Tectonics* (edited by H. M. Prichard, T. Alabaster, N. B. Harris and C. R. Neary), Geol. Soc. Sp. Publ. 76, pp. 427–442, 1993.

McGovern, P. J. and Solomon, S. C., State of stress, faulting, and eruption characteristics of large volcanoes on Mars. *J. Geophys. Res.* **98**(E12), 23553–23579, 1993.

McKenzie, D., Some remarks on the development of sedimentary basins. *Earth Planet. Sci. Lett.* **40,** 25–32, 1978.

McKenzie, D., A possible mechanism for epeirogenic uplift. *Nature* **307,** 616–618, 1984.

McKenzie, D. and Bickle, M. J., The volume and composition of melt generated by extension of the lithosphere. *J. Petrol.* **29**(3), 625–679, 1988.

McKenzie, D. and O'Nions, R. K., Partial melt distributions from inversion of rare earth element concentrations. *J. Petrol.* **32,** 1021–1091, 1991.

Masson, P., Structure pattern analysis of the Noctis Labyrinthus–Valles Marineris region of Mars. *Icarus* **30,** 49–62, 1977.

Masson, P., Contribution to the structural interpretation of the Valles Marineris–Noctis Labyrinthus–Claritas Fossae regions of Mars. *Moon Planets* **22,** 211–219, 1980.

Masson, P., Origin and evolution of the Valles Marineris region of Mars. *Adv. Space Res.* **5**(8), 83–92, 1985.

Mastin, L. G. and Pollard, D. D., Surface deformation and shallow dike intusion processes at Inyo craters, Long Valley, California. *J. Geophys. Res.* **93**(B11), 13221–13235, 1988.

Maurin, J. C. and Guiraud, R., Basement control in the development of the Early Cretaceous West and Central African Rift System. *Tectonophysics* **228,** 81–95, 1993.

Mège, D., Etude morphostructurale de la partie ouest de Valles Marineris (Mars), part II: Interprétation géomorphologique et tectonique. Mémoire de DEA, Laboratoire de géologie dynamique interne, 70 pp., Université Paris XI, Orsay, France, 1991.

Mège, D., Aspects struturaux du complexe magmato-tectonique de Tharsis sur Mars, Thèse de doctorat, Laboratoire de Géologie Dynamique de la Terre et des Planètes, Université Paris-Sud, Orsay, France, 1994.

Mège, D. and Masson, P., Past and current geometry of Valles Marineris, Abstract, EGS XIX General Assembly, Grenoble, 25–29 avril 1994. *Annales Geophysicae* **12** (Suppl. IIIC), 653, 1994a.

Mège, D. and Masson, P., Dans quelles limites peut-on comparer Valles Marineris et les rifts terrestres continentaux? French

extended abstract with English abstract, *Proc. Colloque national de planétologie* (edited by B. R. Bernhard, M. D. Festou and F. Foucaud), pp. S8–42. Institut National des Sciences de l'Univers (CNRS), Toulouse, France, June 13–16, 1994b.

Mège, D. and Masson, P., The Tharsis dyke swarms on Mars. Abstract, EGS XX General Assembly, Hamburg, 3–7 avril 1995. *Annales Geophysicae* **13** (Suppl. IIIC), 749, 1995a.

Mège, D. and Masson, P., Dyke swarms in the Tharsis province of Mars, in *Program and Abstracts, 3rd Int. Dyke Conf.* (edited by A. Agnon and G. Baer), p. 44, Jerusalem, September 4–8, 1995b.

Mège, D. and Masson, P., Stress models for Tharsis formation, Mars. *Planet. Space Sci.* 1996a (in press).

Mège, D. and Masson, P., A plume tectonics model for the Tharsis province, Mars. *Planet. Space Sci.* 1996b (in press).

Melosh, H. J., *Impact Cratering—a Geologic Process*, Oxford Monography on Geology and Geophysics 11, 245 pp. Oxford University Press, Oxford, 1989.

Melosh, H. J. and Williams Jr, C. A., Mechanics of graben formation in crustal rocks: a finite element analysis. *J. Geophys. Res.* **94**(B10), 13961–13973, 1989.

Mercier, J. L., Tapponnier, P., Armijo, R., Han, T. and Zhou, J., Failles normales actives au Tibet: preuves de terrain. *Proc. Coll. franco-chinois sur le Tibet*, pp. 413–422. CNRS, Gif-sur-Yvette, France, May 1981.

Morley, C. K., Evolution, detachments, and sedimentation in continental rifts with particular reference to East Africa. *Tectonics* **8,** 1175–1192, 1989.

Muller, J. P., Iliffe, J., Day, T. and Cook, A. C., EXODUS (Extra-terrestrial Orbital DEMs for Understanding Surfaces) project: automated mapping for comparative planetology, Final Report, 1993.

Mutch, T. A., Arvidson, R. E., Head, J. W., Jones, K. L. and Saunders, R. S., *The Geology of Mars*, 400 pp. Princeton University Press, Princeton, New Jersey, 1976.

Nash, D. B., Morphologic dating of degraded normal fault scarps. *J. Geol.* **88,** 353–360, 1980.

Nedell, S. S., Sedimentary geology of the Valles Marineris, Mars and Antarctic dry valleys lakes, NASA Technical Memorandum 89871, part II, pp. 269–444, 1987.

Neukum, G. and Wise, D. U., Mars: a standard crater curve and possible new time scale. *Science* **194,** 1381–1387, 1976.

Nur, A., The origin of tensile fracture lineaments. *J. Struct. Geol.* **4**(1), 31–40, 1982.

Nur, A., Ron, H. and Scotti, O., Fault mechanics and the kinematics of block rotations. *Geology* **14**(9), 746–749, 1986.

Opheim, J. A. and Gudmundsson, A., Formation and geometry of fractures, and related volcanism, of the Krafla fissure swarm, northeast Iceland. *Geol. Soc. Am. Bull.* **101,** 1608–1622, 1989.

Parsons, T. and Thompson, G. A., Does magmatism influence low-angle normal faulting? *Geology* **21,** 247–250, 1993.

Paterson, M. S., Experimental rock deformation—the brittle field, in *Minerals and Rocks*, Vol. 13, p. 254. Springer, Berlin, 1978.

Peulvast, J. P. and Masson, P., Melas Chasma: morphology and tectonic patterns in central Valles Marineris (Mars). *Earth Moon Planets* **61,** 219–248, 1993.

Peulvast, J. P., Mège, D., Chiciak, J., Costard, F. M. and Masson, P., Very high wallslopes in Valles Marineris (Mars): morphology, evolution, relationships with tectonics and volatiles. *Geomorphology* 1996 (in press).

Phillips, R. J., Saunders, R. S. and Conel, J. E., Mars: crustal structure inferred from Bouguer gravity anomalies. *J. Geophys. Res.* **78**(23), 4815–4820, 1973.

Phillips, R. J., Sleep, N. H. and Banerdt, W. B., Permanent uplift in the magmatic systems with application to the Tharsis region of Mars. *J. Geophys. Res.* **95**(B4), 5089–5100, 1990.

Pike, R. J., Size-dependence in the shape of fresh impact craters on the moon, in *Impact and Erosion Cratering* (edited by D. J. Roddy, R. O. Pepin and R. B. Merrill), pp. 489–509, 1977.

Piper, D. P., Lineament analysis of the environs of the Malawi Rift and the influence of pre-existing structures on rift morphology. *J. Afr. Earth Sci.* **9**(3/4), 579–587, 1989.

Plescia, J. B., Graben and extension in northern Tharsis, Mars. *J. Geophys. Res.* **96**(E3), 18883–18895, 1991.

Plescia, J. B. and Golombek, M. P., Origin of planetary wrinkle ridges based on the study of terrestrial analogs. *Geol. Soc. Am. Bull.* **97,** 1289–1299, 1986.

Plescia, J. B. and Saunders, R. S., Tectonic history of the Tharsis region of Mars. *J. Geophys. Res.* **87**(B12), 9775–9791, 1982.

Pollard, D. D., Elementary fracture mechanics applied to the structural interpretation of dykes, in *Mafic Dyke Swarms* (edited by H. C. Halls and W. F. Fahrig), *Proc. Int. Conf.*, Erindale College, Univ. Toronto, June 4–7, 1985, Geol. Assoc. Canada Sp. Pap. 34, pp. 5–24, 1987.

Price, N. J. and Cosgrove, J. W., *Analysis of Geological Structures*, 502 pp. Cambridge University Press, London, 1990.

Pruis, M. J. and Tanaka, K. L., The Martian northern plains did not result from plate tectonics. *Lunar Planet. Sci. Conf.*, Vol. XXVI, pp. 1147–1148. Lunar and Planetary Institute, Houston, 1995.

Rosendahl, B. R., Architecture of continental rifts with special reference to East Africa. *Ann. Rev. Earth Planet. Sci.* **15,** 445–503, 1987.

Rubin, A. M., A comparison of rift-zone tectonics in Iceland and Hawaii. *Bull. Volcanol.* **52,** 302–319, 1990.

Schubert, G., Solomon, S. C., Turcotte, D. L., Drake, M. J. and Sleep, N. H., Origin and thermal evolution of Mars, in *Mars* (edited by W. S. Kiefer *et al.*), pp. 147–183. Univ. Arizona Press, Tucson, 1992.

Schultz, P. H. and Glicken, H., Impact crater and basin control of igneous processes on Mars. *J. Geophys. Res.* **84,** 8033–8047, 1979.

Schultz, R. A., Structural development of Coprates Chasma and western Ophir Planum, Valles Marineris Rift, Mars. *J. Geophys. Res.* **96**(E5), 22777–22792, 1991.

Schultz, R. A., Limitations on the applicability of Byerlee's law and the Griffith criterion to shallow crustal conditions. *Lunar Planet. Sci. Conf.*, Vol. XXIII, pp. 1239–1240. Lunar and Planetary Institute, Houston, 1992.

Schultz, R. A., Brittle strength of basaltic rock masses with applications to Venus. *J. Geophys. Res.* **98**(E6), 10883–10895, 1993.

Schultz, R. A., Gradients in extension and strain at Valles Marineris, Mars. *Planet. Space Sci.* **43,** 1561–1566, 1995.

Schultz, R. A. and Frey, H. V., A new survey of multiring impact basins on Mars, *Proc. 4th International Conference on Mars. J. Geophys. Res.* **95**(B9), 14175–14189, 1990.

Schultz, R. A. and Senske, D. A., Relationship between uplift, faulting, and strain across Valles Marineris, Mars. *Lunar Planet. Sci. Conf.*, Vol. XXVI, pp. 1253–1254, 1995.

Schultz, R. A. and Tanaka, K. L., Lithospheric-scale buckling and thrust structures on Mars: the Coprates rise and south Tharsis ridge belt. *J. Geophys. Res.* **99**(E4), 8371–8385, 1994.

Schultz, R. A. and Zuber, M. T., Why are strike-slip faults that are "predicted" by lithospheric deformation models rarely observed on planetary surfaces?, in *Lunar Planet. Sci. Conf.*, Vol. XXIII, pp. 1247–1248. Lunar and Planetary Institute, Houston, 1992.

Schultz, R. A. and Zuber, M. T., Observations, models, and mechanisms of failure of surface rocks surrounding planetary loads. *J. Geophys. Res.* **99**(E7), 14691–14702, 1994.

Scott, D. H. and Tanaka, K. L., Geologic map of the western equatorial region of Mars (1:15 M), *U.S. Geol. Survey Misc. Invest. Ser.*, map I-1802-A, 1986.

Sheridan, M. F. and Wohletz, K. H., Hydrovolcanic explosions: the systematics of water–pyroclast equilibration. *Science* **212,** 1387–1389, 1981.

Sleep, N. H. and Phillips, R. J., Gravity and lithospheric stress on the terrestrial planets with reference to the Tharsis region of Mars. *J. Geophys. Res.* **90**(B6), 4469–4489, 1985.

Smith, D. E., Lerch, F. J., Nerem, R. S., Zuber, M. T., Patel, G. B., Fricke, S. K. and Lemoine, F. G., An improved gravity model for Mars: Goddard Mars model 1. *J. Geophys. Res.* **98**(E11), 20871–20889, 1993.

Solomon, S. C. and Chaiken, J., Thermal expansion and thermal stress in the Moon and terrestrial planets: clue to early thermal history. *Proc. 7th Lunar Sci. Conf.*, pp. 3229–3243. Lunar and Planetary Institute, Houston, 1976.

Solomon, S. C. and Head, J. W., Evolution of the Tharsis province of Mars: the importance of heterogeneous lithospheric thickness and volcanic construction: *Proc. 3rd Int. Colloquium on Mars. J. Geophys. Res.* **87**(B12), 9755–9774, 1982.

Squyres, S. W., Wilhelms, D. E. and Moosman, A. C., Large-scale volcano–ground ice interactions on Mars. *Icarus* **70**, 385–408, 1987.

Tanaka, K. L., The stratigraphy of Mars, *Proc. 17th Lunar Planet. Conf. J. Geophys. Res.* **91**(B13), E139–E158, 1986.

Tanaka, K. L. and Davis, P. A., Tectonic history of the Syria Planum province of Mars. *J. Geophys. Res.* **93**(B12), 14893–14917, 1988.

Tanaka, K. L. and Dohm, J. M., Volcanotectonic provinces of the Tharsis region of Mars: identification, variations, and implications, in MEVTV Workshop on Early Tectonic Features on Mars, LPI Technical Rept 89-04 (edited by H. V. Frey), pp. 79–81. Lunar and Planetary Institute, Houston, 1989.

Tanaka, K. L. and Dohm, J. M., Geologic history of the Thaumasia region of Mars. *Lunar Planet. Sci. Conf.*, Vol. XXV, pp. 331–332. Lunar and Planetary Institute, Houston, 1994.

Tanaka, K. L. and Golombek, M. P., Martian tension fractures and the formation of grabens and collapse features at Valles Marineris. *Proc. 19th Lunar Planet. Sci. Conf.*, pp. 383–396, 1989.

Tanaka, K. L. and Golombek, M. P., Strain measurements of impact craters on Tempe Terra, Mars. *Lunar Planet. Sci. Conf.*, Vol. XXV, pp. 1333–1378. Lunar and Planetary Institute, Houston, 1994.

Tanaka, K. L., Golombek, M. P. and Banerdt, W. B., Reconciliation of stress and structural histories of the Tharsis region of Mars. *J. Geophys. Res.* **96**(E1), 15617–15633, 1991.

Toksöz, M. N. and Hsui, A. T., Thermal history and evolution of Mars. *Icarus* **34**, 537–547, 1978.

U.S. Geological Survey, Topographic orthophoto mosaic of the Tithonium Chasma region of Mars (1:500 K), *U.S. Geol. Survey Misc. Invest. Ser.*, map I-1294, 1980.

U.S. Geological Survey, Topographic map of the Coprates Northwest quadrangle of Mars (1:2,000,000), *U.S. Geol. Survey Misc. Invest. Ser.*, map I-1712, 1986.

U.S. Geological Survey, Topographic maps of the polar, western, and eastern regions of Mars (1:15 M), *U.S. Geol. Survey Misc. Invest. Ser.*, map I-2160, 1991.

U.S. Geological Survey, Mars digital topographic map vol. 7, Global topography, CDROM VO 2007, 1992.

van der Beek, P., Cloetingh, S. and Andriessen, P., Mechanisms of extensional basin formation and vertical motions at rift flanks: constraints from tectonic modelling and fission-track thermochronology. *Earth Planet. Sci. Lett.* **121**, 417–433, 1994.

Villeneuve, M., Les sillons tectoniques du Précambrien supérieur dans l'est du Zaïre; comparaisons avec les directions du rift est-africain, in *Rifts et fossés anciens* (edited by M. Popoff and J. J. Tiercelin). *Bull. Centre Rech. Explor.-Prod. Elf-Aquitaine* **7**(1), 163–174, 1983.

Wallace, R. E., Profiles and ages of young fault scarps, North-Central Nevada. *Geol. Soc. Am. Bull.* **88**, 1267–1281, 1977.

Wallace, R. E., Geometry and rates of change of fault-generated range fronts, north-central Nevada. *J. Res. U.S. Geol. Surv.* **6**(5), 637–650, 1978.

Ward, A. W., Yardangs on Mars: evidence of recent wind erosion. *J. Geophys. Res.* **84**(B14), 8147–8166, 1979.

Watters, T. R., Compressional tectonism on Mars. *J. Geophys. Res.* **98**(E9), 17049–17060, 1993.

Watters, T. R. and Maxwell, T. A., Orientation, relative age, and extent of the Tharsis plateau ridge system. *J. Geophys. Res.* **91**, 8113–8125, 1986.

Weissel, J. K. and Karner, G. D., Flexural uplift of rift flanks due to mechanical unloading of the lithosphere during extension. *J. Geophys. Res.* **94**(B10), 13919–13950, 1989.

Wernicke, B., Uniform-sense normal simple shear of the continental lithosphere. *Can. J. Earth Sci.* **22**, 108–125, 1985.

White, R. and McKenzie, D., Magmatism at rift zones: the generation of volcanic continental margins and flood basalts. *J. Geophys. Res.* **94**(B6), 7685–7729, 1989.

Willemann, R. J. and Turcotte, D., The role of lithospheric stress in the support of the Tharsis rise, *Proc. 3rd Int. Colloquium on Mars. J. Geophys. Res.* **87**(B12), 9793–9801, 1982.

Wise, D. U., Golombek, M. P. and McGill, G. E., Tectonic evolution of Mars. *J. Geophys. Res.* **84**(B14), 7934–7939, 1979.

Witbeck, Tanaka, K. L. and Scott, D. H., Geologic map of the Valles Marineris region, Mars (1:2 M), *U.S. Geol. Survey Misc. Invest. Series*, map I-2010, 1991.

Ziegler, P. A., European rift system. *Tectonophysics* **208**, 91–111, 1992a.

Ziegler, P. A., North Sea rift system. *Tectonophysics* **208**, 55–75, 1992b.

Zoback, M. L., First- and second-order patterns of stress in the lithosphere: the World Stress Map project. *J. Geophys. Res.* **97**(B8), 11703–11728, 1992.

Zoback, M. L. and Richardson, R. M., Stress perturbation associated with the Amazonas and other ancient continental rifts. *J. Geophys. Res.* **101**, 5459–5475, 1996.

Zuber, M. T., Wrinkle ridges, reverse faulting, and the depth penetration of lithospheric strain in Lunae Planum, Mars. *Icarus* **114**, 80–92, 1995.